Life histories and niche dynamics in late Quaternary proboscideans from Midwestern North America: evidence from stable isotope analyses

Chris Widga[1,2], Greg Hodgins[3], Kayla Kolis[4], Stacey Lengyel[1,2], Jeff Saunders[2,5], J. Douglas Walker[6], Alan D. Wanamaker[7]

Affiliations

1. Don Sundquist Center of Excellence in Paleontology, East Tennessee State University, Johnson City, TN

2. Illinois State Museum, Springfield, IL

3. Department of Physics, University of Arizona, Tucson, AZ

4. Biodiversity Institute, University of Kansas, Lawrence, KS

5. The Desert Laboratory on Tumamoc Hill, University of Arizona, Tucson, AZ

6. Department of Geology, University of Kansas, Lawrence, KS

7. Department of Geological and Atmospheric Sciences, Iowa State University, Ames, IA

Key Words: Mammoths, Mastodons, Stable Isotopes, Paleoecology, Midwest, Mobility

ABSTRACT

Stable isotopes of mammoths and mastodons have the potential to illuminate ecological changes in late Pleistocene landscapes and megafaunal populations as these species approached extinction. The ecological factors at play in this extinction remain unresolved, but isotopes of bone collagen ($\delta^{13}C$, $\delta^{15}N$) and tooth enamel ($\delta^{13}C$, $\delta^{18}O$, $^{87}Sr/^{86}Sr$) from the Midwest, USA are leveraged to examine ecological and behavioral changes that occurred during the last interglacial-glacial cycle. Both species had significant C3 contributions to their diets and experienced increasing levels of niche overlap as they approached extinction. A subset of mastodons after the last glacial maximum (LGM) exhibit low $\delta^{15}N$ values that may represent expansion into a novel ecological niche, perhaps densely occupied by other herbivores. Stable isotopes from serial and micro-sampled enamel show increasing seasonality and decreasing temperatures as mammoths transitioned from Marine Isotope Stage (MIS) 5e to glacial conditions (MIS 4, MIS 3, MIS 2). Isotopic variability in enamel suggests mobility patterns and life histories have potentially large impacts on the interpretation of their stable isotope ecology. This study further refines the ecology of midwestern mammoths and mastodons demonstrating increasing seasonality and niche overlap as they responded to landscape changes in the final millennia before extinction.

INTRODUCTION

Historically, the late Quaternary record of mammoths and mastodons in the Midwest has played an important role in understanding megafaunal extinctions in North America (e.g., Fisher 2008, 2018; Graham et al., 1981; Saunders et al. 2010; Widga et al., 2017a; Yansa and Adams, 2012). Whether extinctions are viewed as human-induced (Mosimann and Martin 1975; Alroy 2001; Surovell et al. 2005; Fisher 2009; Surovell et al. 2016), the result of late Pleistocene landscape changes (Stuart et al. 2004; Nogués-Bravo et al. 2008; Widga et al. 2017a), a function of other ecological processes (Ripple and Van Valkenburgh 2010), or some combination, this region is unparalleled in its density of large, late Quaternary vertebrates and associated paleoecological localities. For these reasons, the midcontinent has proven critical to understanding ecological dynamics in proboscidean taxa leading up to extinction. In recent years, it has been recognized that multiple proboscidean taxa shared an ecological niche in late Pleistocene landscapes (Saunders et al. 2010) despite distinct extinction trajectories (Widga et al. 2017a). Chronological studies indicate that proboscideans in this region experienced extinction *in situ*, rather than mobilizing to follow preferred niche space (Saunders et al. 2010). Despite refinements in our understanding of mammoths and mastodons in the region, many significant questions remain. Modern megafauna have a profound impact on local vegetation (Guldemond and Van Aarde 2008; Valeix et al. 2011), and it is unclear what effect late Pleistocene mammoths and mastodons would have had on canopy cover, nutrient cycling, and fruit dispersal in non-analogue vegetation communities. There are still issues of equifinality in how the presence of human predators (Fisher 2009) or the virtual absence of both humans and large carnivores (Widga et al. 2017a) impacted proboscidean populations in the region as they neared extinction.

The high profile debate surrounding the cause of late Pleistocene megafaunal extinctions has spurred a number of productive regional studies to address the timing and paleoecology of extinction in megafaunal taxa (Pacher and Stuart 2009; Stuart and Lister 2011, 2012; Stuart 2015; Widga et al. 2017a). The results of this research serve to constrain the number of possible extinction scenarios and to highlight the need for regional-scale and taxon-specific analyses.

As in modern ecosystems, Proboscidea in late Pleistocene North America were long-lived taxa that likely had a profound impact on the landscape around them. Due to their size and energetic requirements, elephantoids are a disruptive ecological force, promoting open canopies in forests through tree destruction (Chafota and Owen-Smith 2009) and trampling vegetation (Plumptre 1994). Their dung is a key component of soil nutrient cycling (Owen-Smith 1992; Augustine et al. 2003), and was likely even more important in N limited tundra and boreal forest systems of temperate areas during the late Pleistocene. Even in death, mammoths and mastodons probably wrought major changes on the systems within which they were interred (Coe 1978; Keenan et al. 2018) providing valuable nutrient resources to scavengers and microbial communities. Precisely because proboscideans play such varied and important roles in the ecosystems they inhabit, they are good study taxa to better understand Pleistocene ecosystems. They are also central players in many extinction scenarios.

One of the major challenges to ecological questions such as these is scale (Delcourt and Delcourt 1991; Denny et al. 2004; Davis and Pineda-Munoz 2016). Processes that are acting at the level of an individual or a locality can vary significantly in space and time (Table 1). Paleoecological data collected from individual animals from local sites is constrained by larger regional patterns that may or may not be apparent (e.g., taphonomic contexts, predator-prey dynamics). Paleoecological studies of vertebrate taxa often begin with the premise that the

83 individual is an archive of environmental phenomena experienced in life. In long-lived taxa such
84 as proboscideans, this window into past landscapes may span many decades. This longevity is
85 both a benefit and a challenge to studies of proboscidean paleoecology.

86 Table 1. Scales of paleoecological analysis.

Scale	Method	Phenomena	Selected References
Small (Days)	Stomach contents, enamel micro-wear	Animal health, Landscape (local scale)	Rhodes et al. 1998; Teale and Miller 2012; Green, DeSantis, and Smith 2017; Smith and DeSantis 2018.
Meso (Weeks-Months)	Hair, Tusk/Tooth dentin, Tooth enamel	Seasonal diets, Reproductive events (e.g., musth, calving), Migration/Dispersal	Fox and Fisher 2001; Hoppe 2004; Hoppe and Koch 2007; Cerling et al. 2009; Metcalfe and Longstaffe 2012; Fisher 2018
Large (Years - Decades)	Bone collagen, tooth enamel, tooth mesowear	Climate/Vegetation trends, Large-scale land-use trends, Population-level trends in diet responses to landscape changes.	Bocherens et al. 1996; Iacumin et al. 2010; Szpak et al. 2010

87

88 Some approaches offer relatively high-resolution snapshots of animal ecology at a scale
89 that is of a short duration (days). Micro-wear analyses of dentin and enamel (Green et al. 2017;
90 Smith and DeSantis 2018) are increasingly sophisticated, and have the potential to track short-
91 term dietary trends. The remains of stomach contents also provide ecological information at this
92 scale (Lepper et al. 1991; Newsom and Mihlbachler 2006; van Geel et al. 2011; Fisher et al.
93 2012; Teale and Miller 2012; Birks et al. 2019), which are essentially the 'last meal' representing
94 a few hours of individual browsing. These techniques offer paleoecological insights that are
95 minimally time-averaged, and at a timescale that may be comparable to modern observations of
96 animal behavior.

97 Other approaches resolve time periods that are weeks to months in duration. Fisher's
98 (Fisher and Fox 2006; Fisher 2009; 2018) work on incremental growth structures in
99 proboscidean tusk and molar dentin reliably record weekly to monthly behaviors. The resolution

of these methods may even include short-term, often periodic, life history events, such as reproductive competition (musth) and calving. Other researchers (Hoppe et al. 1999; Metcalfe and Longstaffe 2012; 2014; Pérez-Crespo et al. 2016) have explored incremental growth trends in proboscidean tooth enamel. Adult molars form over the course of 10-12 years with an enamel extension rate of ~1 cm/year in both modern elephants (Uno et al. 2013) and mammoths (Dirks et al. 2012; Metcalfe and Longstaffe 2012) providing the opportunity to understand meso-scale (potentially monthly) changes in diet and behavior.

Finally, some techniques measure animal diet and behavior over much longer scales (years-decades). In humans, bone collagen is replaced at a rate of 1.5-4% per year (Hedges et al. 2007). For equally long-lived proboscidean taxa, this means that stable isotope analyses of bone collagen is essentially sampling a moving average of ~20 years of animal growth. For younger age groups, this average will be weighted towards time periods of accelerated maturation (adolescence), when collagen is replaced at a much greater rate (Hedges et al. 2007). Tooth enamel can also be sampled at a resolution (i.e., "Bulk" enamel) that averages a year (or more) of growth (Hoppe 2004; Baumann and Crowley 2015), and it is likely that this is the approximate temporal scale that is controlling tooth mesowear (Fortelius and Solounias 2000).

Stable isotope studies are an important part of the paleoecological toolkit for understanding Quaternary proboscideans and are capable of resolving animal behavior at multiple timescales. Progressively larger, more complete datasets characterize isotopic studies of Beringian mammoths, where stable carbon and oxygen isotopes in bone collagen and tooth enamel reliably track climate and landscape changes over the late Pleistocene (Bocherens et al. 1996; Iacumin et al. 2010; Szpak et al. 2010; Arppe et al. 2019), the place of mammoths in

122 regional food webs (Fox-Dobbs et al. 2007, 2008), and characteristics of animal growth and
123 maturation (Metcalfe and Longstaffe 2012; Rountrey et al. 2012; El Adli et al. 2017).

124 These studies have also been important to understanding both lineages of proboscideans
125 in temperate North America. From the West Coast (Coltrain et al. 2004; El Adli et al. 2015) to
126 the southwestern (Metcalfe et al. 2011), and eastern US (Koch et al. 1998; Hoppe and Koch
127 2007), isotopic approaches have been very successful in understanding local to regional scale
128 behavior in mammoths and mastodons. Although there have been efforts to understand
129 mammoth and mastodon behaviors in the Midwest at relatively limited geographic scales
130 (Saunders et al. 2010; Baumann and Crowley 2015), there is a need to systematically address
131 long-term isotopic trends throughout the region. In this paper, we approach this problem from a
132 broad regional perspective, leveraging a recently reported radiocarbon (^{14}C) dataset with
133 associated isotopic data on bone collagen. We also utilize an enamel dataset consisting of both
134 serial bulk and micro-milled mammoth molar enamel samples (C, O, Sr isotope systems).
135 Together, the results of these analyses offer a picture of mammoth and mastodon diets ($\delta^{13}C$,
136 $\delta^{15}N$), late Quaternary paleoclimate ($\delta^{18}O$), and animal mobility ($^{87}Sr/^{86}Sr$) that is geographically
137 comprehensive and spans the past 50,000 years.

138 ## MATERIALS AND METHODS

139 The proboscidean dataset in this study (Figure 1; SM Table 1, SM Table 2, SM Table 3)
140 was acquired with the goal of understanding mammoth and mastodon population dynamics
141 during the late Pleistocene as these taxa approach extinction. Chronological and broad-scale
142 paleoecological implications for this dataset were explored in Widga et al. (2017a) and more
143 recently in Broughton and Weiztel (2018). In this paper we focus on the implications of these

144 data for the stable isotope ecology of midwestern Proboscidea. We also discuss annual patterns
145 in five serially sampled mammoth teeth spanning the last glacial-interglacial cycle. Finally, we
146 micro-sampled two mammoths from the Jones Spring locality in Hickory Co., MO. Although
147 beyond the range of radiocarbon dating, both samples are associated with well-dated
148 stratigraphic contexts (Haynes 1985). Specimen 305JS77 is an enamel ridge-plate recovered
149 from unit d1 (spring feeder), refitting to an M3 from unit c2 (lower peat). Unit c2 is part of the
150 lower Trolinger formation (Haynes 1985) and can be assigned to Marine Isotope Stage (MIS) 4.
151 Specimen 64JS73 is an enamel ridge-plate from unit e2 (sandy peat) in the upper Trolinger
152 formation (Haynes 1985) and can be assigned to MIS 3. Together, these samples provide dozens
153 of seasonally-calibrated isotopic snapshots representing mammoth behavior from individuals that
154 pre-date the last glacial maximum (LGM).

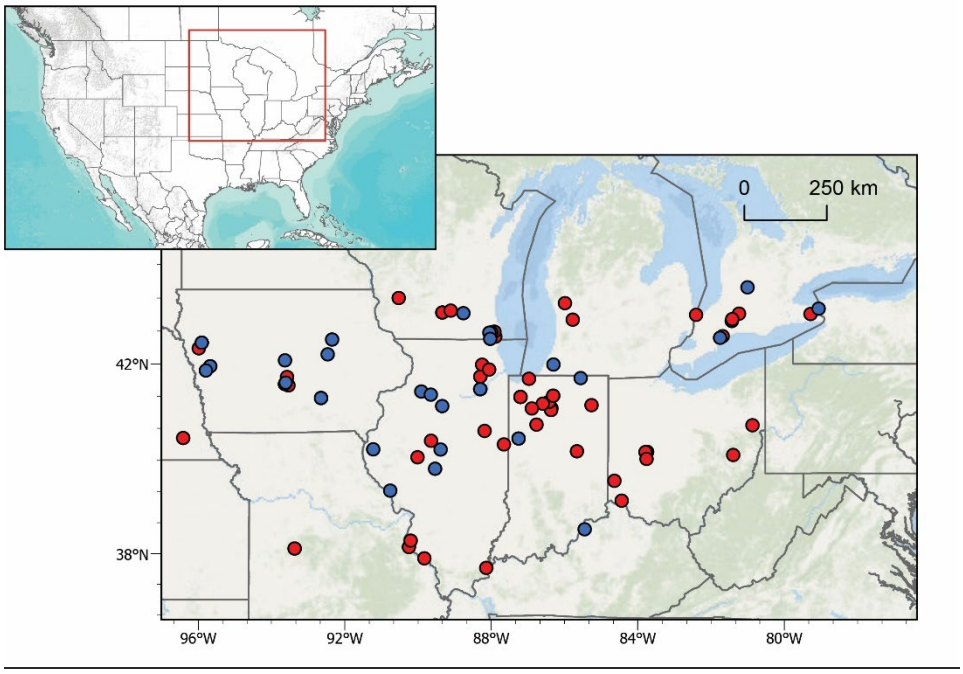

155

156 Figure 1. Map of dated midwestern mammoths (blue) and mastodons (red) with associated
157 $\delta^{13}C_{coll}$ and $\delta^{15}N_{coll}$ data. See SM Table 2 for details.

158

159 Mammoth and Mastodon bone collagen. Proboscidean samples were selected to widely
160 sample midwestern Proboscidea, both stratigraphically and geographically (Widga et al. 2017a).
161 Due to extensive late Pleistocene glaciation in the region, this dataset is dominated by samples
162 dating to the LGM or younger (<22 ka). Only 14 out of 93 (15%) localities predate the LGM.

163 All samples were removed from dense bone, tooth or tusk dentin and submitted to the
164 University of Arizona AMS laboratory. Collagen was prepared using standard acid-base-acid
165 techniques (Brock et al. 2010), its quality evaluated visually, and through ancillary
166 Carbon:Nitrogen (C:N) analyses. Visually, well-preserved collagen had a white, fluffy
167 appearance and C:N ratios within the range of modern bones (2.9-3.6) (Tuross et al. 1988).
168 Samples outside of this range were not included in the study. Samples that had the potential to be
169 terminal ages were subjected to additional analyses where the ABA-extracted gelatin was ultra-
170 filtered (UF) through >30 kD syringe filters to isolate relatively undegraded protein chains
171 (Higham et al. 2006). This fraction was also dated. All radiocarbon ages in this dataset are on
172 collagen from proboscidean bone or tooth dentin and available in Widga et al. (2017a), through
173 the Neotoma Paleoecology Database (www.neotomadb.org) or in SM Table 1. Measured
174 radiocarbon ages were calibrated in Oxcal v4.3 (Bronk Ramsey 2009) using the Intcal13 dataset
175 (Reimer et al. 2013). All stable isotope samples were analyzed on a Finnigan Delta PlusXL
176 continuous-flow gas-ratio mass spectrometer coupled to a Costech elemental analyzer at the
177 University of Arizona. Standardization is based on acetanilide for elemental concentration, NBS-
178 22 and USGS-24 for $\delta^{13}C$, and IAEA-N-1 and IAEA-N-2 for $\delta^{15}N$. Isotopic corrections were
179 done using a regression method based on two isotopic standards. The long-term analytical
180 precision (at 1σ) is better than ± 0.1‰ for $\delta^{13}C$ and ± 0.2‰ for $\delta^{15}N$. All $\delta^{13}C$ results are

reported relative to Vienna Pee Dee Belemnite (VPDB) and all $\delta^{15}N$ results are reported relative to N-Air.

Serial and Micro-sampling of Mammoth tooth enamel. Mammoth enamel ridge-plates were sampled at two different scales. Serial sampling consisted of milling a series of 5-10 mg samples of enamel powder with a handheld rotary tool equipped with a 1.5 mm diameter carbide bit along the axis of growth. Sample spacing was ~1 sample per centimeter of tooth growth. However, given the geometry and timing of enamel maturation (Dirks et al. 2012), these samples at best, approximate an annual scale of dietary and water inputs.

Micro-sampling however, has the potential to record sub-annual patterns in animal movement and behavior (Metcalfe and Longstaffe 2012). For this project, we built a custom micromill capable of *in situ*, micron-resolution, vertical sampling of a complete mammoth molar. This micromill setup consisted of two Newmark linear stages coupled to a Newmark vertical stage to allow movement in 3-dimensions. These stages were controlled by a Newmark NSC-G 3-axis motion controller using GalilTools on a PC. A 4-cm diameter ball joint allowed levelling of a metal (Version 1) or acrylic (Version 2) plate for holding a specimen. The armature for Version 1 consisted of a 1971 Olympus Vanox microscope retrofitted with a stationary Proxxon 50/E rotary tool using a 0.5mm end mill. Version 2 has replaced this setup with a U-strut armature using a 3D printed drill mount to allow for greater vertical and horizontal movement to accommodate large, organically-shaped specimens. Specimens were stabilized on the mounting plate using heat-flexible thermoplastic cradle affixed to a metal plate with machine screws (Version 1). However, we later developed an acrylic mounting plate method where a mammoth tooth could be sufficiently stabilized using zip ties (Version 2). This micromill was developed to address the challenges of accurately micro-milling large specimens with minimal instrumentation

costs. Complete plans for this micromill are available under an open hardware license at https://osf.io/8uhqd/?view_only=43b4242623a94a529e4c6ef2396345e9.

Micro-mill sampling resolution was 1 sample per millimeter along the growth axis of the tooth plate (Figure 2). Each sample was milled in 100μm-deep passes through the entire thickness of the enamel. The lowest enamel sample (i.e., closest to the enamel-dentin boundary) in the series was used for isotopic analyses to minimize the effects of mineralization and diagenesis on the biological signal (Zazzo et al. 2006). Enamel powder was collected in de-ionized water to; 1) maximize sample recovery, and 2) lubricate the mill. These samples were too small for standard pretreatment of tooth enamel CO_3 (Koch et al. 1997). However, paired bulk enamel samples treated with 0.1 N acetic acid and 2.5% NaOCl show results that are the same as untreated bulk samples. Although this technique is both time- and labor- intensive, it is minimally invasive and is capable of sampling enamel growth structures at high resolution.

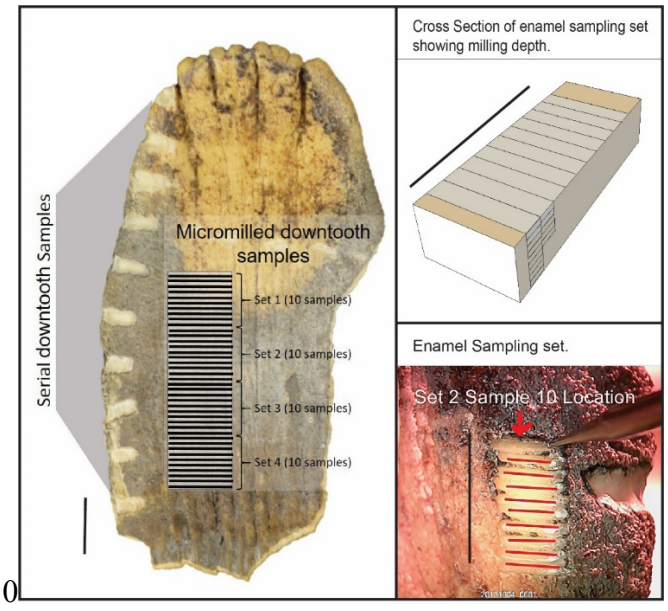

Figure 2. Schematic illustration of serial and micro-sampling strategies. Black bar is equal to 1 cm.

All enamel powder samples were measured in a Finnigan Delta Plus XL mass spectrometer in continuous flow mode connected to a Gas Bench with a CombiPAL autosampler at the Iowa State University Stable Isotope lab, Department of Geological and Atmospheric Sciences. Reference standards (NBS-18, NBS-19) were used for isotopic corrections, and to assign the data to the appropriate isotopic scale. Corrections were done using a regression method using NBS-18 and NBS-19. Isotope results are reported in per mil (‰). The long-term precision (at 1σ) of the mass spectrometer is ±0.09‰ for $\delta^{18}O$ and ±0.06‰ for $\delta^{13}C$, respectively, and precision is not compromised with small carbonate samples (~150 micrograms). Both $\delta^{13}C$ and $\delta^{18}O$ are reported VPDB.

Enamel $\delta^{13}C$ results are corrected -14.1‰ to approximate the $\delta^{13}C$ of dietary input ($\delta^{13}C_{diet}$) (Daniel Bryant and Froelich 1995).

Enamel $\delta^{18}O$ results were converted from VPDB to SMOW using the equation:

$$\delta^{18}O\ SMOW = (1.03086 * \delta^{18}O\ VPDB) + 30.86$$

The $\delta^{18}O$ of enamel phosphate ($\delta^{18}O_p$) for these samples was calculated from the $\delta^{18}O$ of enamel carbonate ($\delta^{18}O_c$) (Fox and Fisher 2001)

$$\delta^{18}O_p = (\delta^{18}O_c/1.106) - 4.7288$$

Estimates of body water $\delta^{18}O$ ($\delta^{18}O_w$) were calculated following Dauxe et al. (2008)

$$\delta^{18}O_w = (1.54 * \delta^{18}O_p) - 33.72$$ (Dauxe et al. 2008)

The $^{87}Sr/^{86}Sr$ component of enamel bioapatite reflects changes in the geochemical makeup of the surface an animal grazed across during tooth formation. In serial-scale analyses,

239 enamel powder samples were split from the light isotope samples described above, and represent
240 the same portions of mammoth teeth. Each ~5 mg sample of powder was leached in 500 µL 0.1
241 N acetic acid for four hours to remove diagenetic calcite and rinsed 3 times with deionized water
242 (centrifuging between each rinse). In the micromilled series, small sample sizes prevented Sr
243 analyses from being performed on the same samples as $\delta^{13}C$ and $\delta^{18}O$ analyses. Therefore, Sr
244 from these growth series was analyzed opportunistically, or at the scale of 1 sample every 2mm.

245 All enamel samples were then dissolved in 7.5 N HNO_3 and the Sr eluted through ion-
246 exchange columns filled with strontium-spec resin at the University of Kansas Isotope
247 Geochemistry Laboratory. $^{87}Sr/^{86}Sr$ ratios were measured on a Thermal Ionization Mass
248 Spectrometer (TIMS), an automated VG Sector 54, 8-collector system with a 20-sample turret, at
249 the University of Kansas Isotope Geochemistry laboratory. Isotope ratios were adjusted to
250 correspond to a value of 0.71250 on NBS-987 for $^{87}Sr/^{86}Sr$. We also assumed a value of $^{86}Sr/^{88}Sr$
251 of 0.1194 to correct for fractionation.

252 The distribution of $^{87}Sr/^{86}Sr$ values in vegetation across the surface of the midcontinent is
253 determined by the values of soil parent material. In a large part of this region, surface materials
254 are composed of allochthonous Quaternary deposits such as loess, alluvium, and glacial debris.
255 Therefore continent-scale Sr isoscape models derived from bedrock or water (Bataille and
256 Bowen 2012) are not ideal for understanding first order variability in midwestern $^{87}Sr/^{86}Sr$. For
257 these reasons, Widga et al. (2017) proposed a Sr isoscape for the Midwest based on surface
258 vegetation. At a regional scale, these trends in vegetation $^{87}Sr/^{86}Sr$ reflect the Quaternary history
259 of the region, and are consistent with other, empirically derived, patterns in Sr isotope
260 distribution from the area (Slater et al. 2014; Hedman et al. 2018). Sr isotope values in mammoth

enamel are compared to a $^{87}Sr/^{86}Sr$ isoscape constructed from the combined datasets of Widga et al. (2017b) and Hedman et al. (2009), and Hedman et al. (2018).

RESULTS

The collagen of 54 mastodons and 22 mammoths was analyzed for $\delta^{13}C_{coll}$ and $\delta^{15}N_{coll}$ (Table 2). Three mastodons have ^{14}C ages that place them beyond the range of radiocarbon dating, and the youngest mastodons date to the early part of the Younger Dryas, shortly before extinction. Despite being well-represented prior to the LGM and during deglaciation (i.e., Oldest Dryas, Bølling, Allerød, Younger Dryas), this dataset lacks mastodons from the study region during the coldest parts of the LGM. Mammoths are present in this dataset from 40 ka until their extinction in the region during the late Allerød.

Visually, there is substantial amounts of overlap in the $\delta^{13}C_{coll}$ and $\delta^{15}N_{coll}$ of mammoths and mastodons through the duration of the dataset (Figure 3, Table 2). Both taxa show average $\delta^{13}C_{coll}$ values around -20‰, consistent with a diet dominated by C3 trees, shrubs, and/or cool-season grasses. This is broadly consistent with variable, but shared diets during time periods when both taxa occupied the region. The average $\delta^{13}C_{coll}$ values for mammoths (-20.4‰) is similar to that of mastodons (-21.0‰). The average $\delta^{15}N_{coll}$ of mammoths (7.5‰) is elevated compared to mastodons (4.4‰).

However, dietary relationships between taxa are not static through time. Prior to the LGM, both $\delta^{13}C_{coll}$ and $\delta^{15}N_{coll}$ are significantly different between mammoths and mastodons ($\delta^{13}C$ t-test; $p=0.013$; $\delta^{15}N$ t-test; $p=0.010$). During the Oldest Dryas the $\delta^{13}C_{coll}$ of both taxa is very similar, although $\delta^{15}N_{coll}$ between mammoths and mastodons remains distinct (t-test; $p=0.012$). During the Allerød, $\delta^{13}C_{coll}$ and $\delta^{15}N_{coll}$ between taxa are indistinguishable.

283 The $\delta^{13}C_{coll}$ signature of mastodon diets changes little throughout the last 50 ka. Despite a
284 noticeable absence of mastodon material during the height of the LGM, the only significant shift
285 in the $\delta^{13}C_{coll}$ of mastodon diets occurs between the Bølling and the Allerød (t-test; p=0.008).
286 Mastodon $\delta^{15}N_{coll}$ values fall clearly into two groups, those that date prior to the LGM,
287 and those that post-date the LGM. Mastodon $\delta^{15}N_{coll}$ values are significantly higher in pre-LGM
288 samples than in samples dating to the Younger Dryas (t-test; p=0.010), Allerød (t-test; p=0.017),
289 and Bølling (t-test; p<0.000). Of note is a group of mastodons that show lower $\delta^{15}N_{coll}$ values
290 during the Oldest Dryas, Bølling, Allerød, and Younger Dryas, when the average $\delta^{15}N_{coll}$ values
291 decrease to values <5‰. A similar shift is not evident in mammoths at this time.
292 Mammoth $\delta^{13}C_{coll}$ during MIS 3 is significantly different from mammoths dating to LGM
293 II (t-test; p=0.008) or the Oldest Dryas (t-test; p=0.005). There are no significant differences in
294 mammoth $\delta^{15}N_{coll}$ between different time periods.
295

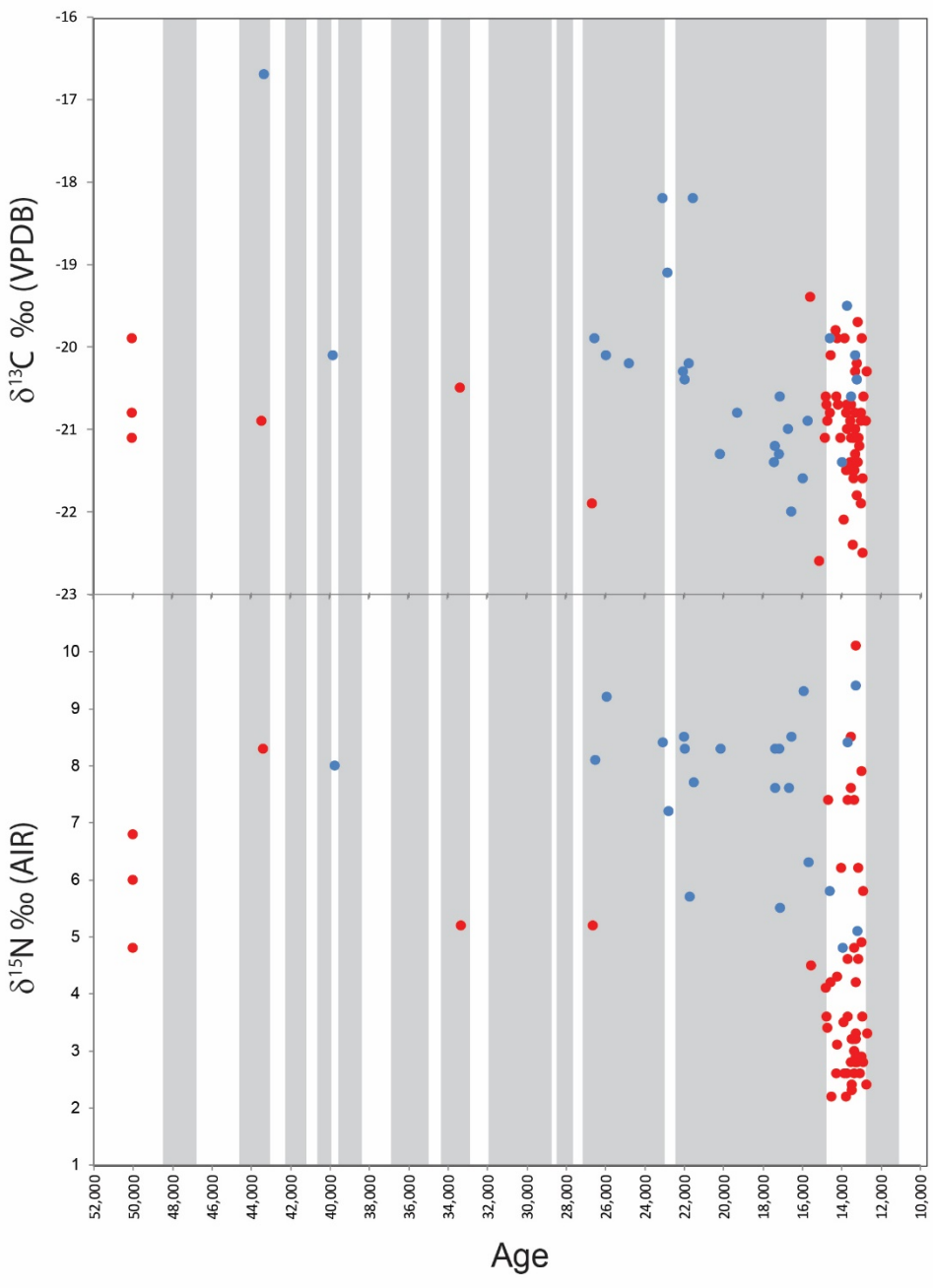

Figure 3. Changes in midwestern proboscidean collagen $\delta^{13}C$ and $\delta^{15}N$ through time. Mastodons=red, Mammoths=blue, glacial stadials = grey bars. Stadial chronology from Rasmussen et al., 2014.

Table 2. Mastodon and Mammoth collagen stable isotope values, by chronozone. $\delta^{13}C$ values reported as ‰ relative to VPDB. $\delta^{15}N$ values reported as ‰ relative to Air.

Taxon	Chronozone	N	$\bar{x}$ $\delta^{13}C$ (s.d)	$\bar{x}$ $\delta^{15}N$ (s.d)
Mammut	Younger Dryas (12.9-11.5 ka)	2	-20.6 (0.4)	2.9 (0.6)
	Allerød (14.0-12.9 ka)	35	-21.1 (0.6)	4.2 (2.1)
	Bølling (14.6-14.0 ka)	6	-20.4 (0.5)	3.8 (1.5)
	Oldest Dryas (14.6-17.4 ka)	5	-20.5 (0.7)	4.6 (1.6)
	LGM II (17.4-20.9 ka)	0		
	LGM I (20.9-22.9 ka)	0		
	Pre-LGM (>22.9 ka)	6	-20.9 (0.7)	6.1 (1.3)
	Average	54	-21.0 (0.7)	4.4 (2.0)
Mammuthus	Allerød (14.0-12.9 ka)	3	-20.6 (0.9)	6.1 (2.0)
	Bølling (14.6-14.0 ka)	1	-19.9	5.8
	Oldest Dryas (14.6-17.4 ka)	4	-21.4 (0.5)	7.9 (1.3)
	LGM II (17.4-20.9 ka)	4	-21.1 (0.4)	7.4 (1.3)
	LGM I (20.9-22.9 ka)	5	-20.1 (1.1)	7.6 (1.2)
	Pre-LGM (>22.9 ka)	5	-19.6 (0.8)	8.2 (0.7)
	Average	22	-20.4 (1.0)	7.5 (1.3)

* $\bar{x}$ = mean; s.d. = standard deviation

All serial enamel series were between 9 and 16 cm in length and represent multiple years. Stable oxygen isotopes of three MIS 2 mammoths (Principia College, Brookings, Schaeffer) overlap significantly, while MIS 4 (234JS75) and MIS 5e (232JS77) mammoths from Jones Spring show elevated values indicative of warmer conditions (Table 3; Figure 4). The variance in serially sampled MIS 2 mammoths (average amp. = 2.5‰) was not significantly different from the series from Jones Spring, dating to MIS 4 (amp. = 2.9‰)(F-test; p=0.320). However, the MIS 5e mammoth from Jones Spring has a smaller amplitude (amp. = 1.1‰) compared to both the MIS 4 mammoth (F-test; p=0.003) and the three MIS 2 mammoths (F-test; p<0.000). Strontium isotope ratios of this animal indicates a home range on older surfaces of the Ozarks, throughout tooth formation, with a period of relatively elevated $^{87}Sr/^{86}Sr$ values also corresponding to low $\delta^{18}O$ values.

317 Table 3. Summary of serial and micro-sampled *Mammuthus* tooth enamel: $\delta^{13}C$, $\delta^{18}O$, and
318 $^{87}Sr/^{86}Sr$.

ID	$\delta^{13}C$				$\delta^{18}O$				$^{87}Sr/^{86}Sr$			
Serial Analyses	X	Min	Max	Amp	X	Min	Max	Amp	X	Min	Max	Amp
Principia College (MIS 2)	-10.9	-11.3	-10.0	1.4	-7.9	-8.7	-6.7	2.0				
Brookings Mammoth (MIS 2)	-9.9	-10.5	-9.4	1.1	-9.2	-10.0	-7.8	2.2				
Schaefer Mammoth (MIS 2)	-9.0	-9.9	-7.0	3.0	-8.3	-9.9	-6.6	3.3				
Jones Sp. Mammoth, 243JS75 (MIS 4)	-1.7	-2.3	-0.2	2.1	-3.4	-4.5	-1.6	2.9				
Jones Sp. Mammoth, 232JS77 (MIS 5e)	-2.8	-3.8	-1.3	2.5	-0.5	-4.6	3.6	1.1	0.7162	0.7146	0.7177	-0.0031
Micro-Analyses												
305JS77 (MIS 5e)	-2.4	-3.5	-0.2	3.3	-3.9	-4.9	-2.9	2.0	0.7109	0.7106	0.7118	-0.0012
64JS73 (MIS 3)	-2.8	-4.3	-1.7	2.6	-4.9	-12.0	-0.4	11.7	0.7152	0.7140	0.7164	-0.0025

319

320 Two mammoth teeth from the Jones Spring locality in Hickory Co., MO were micro-
321 sampled (Figure 5). These specimens are from beds representative of MIS 5e and MIS 3
322 deposits.

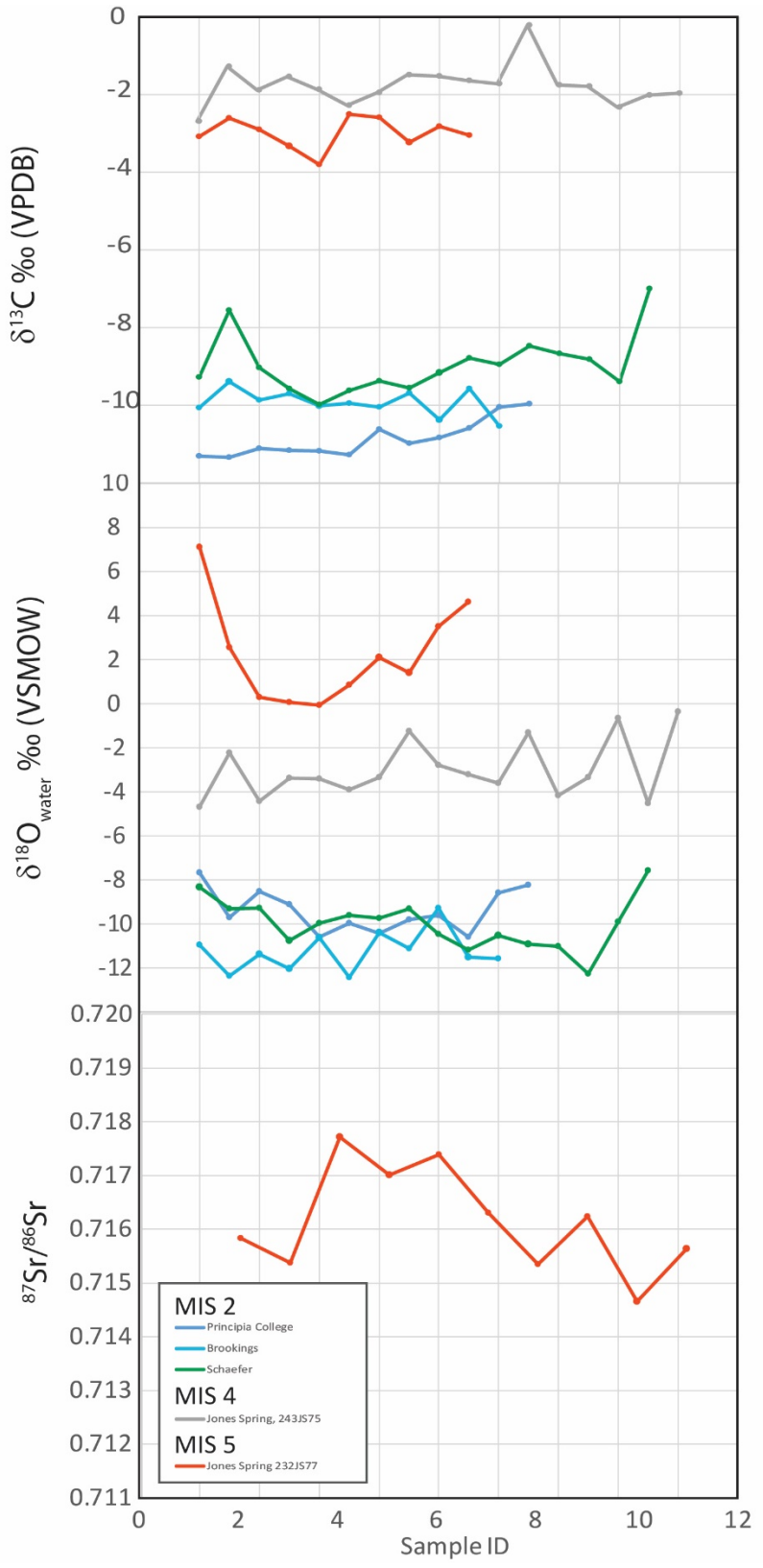

Figure 4. Time series, serial enamel $\delta^{13}C$, $\delta^{18}O$, $^{87}Sr/^{86}Sr$.

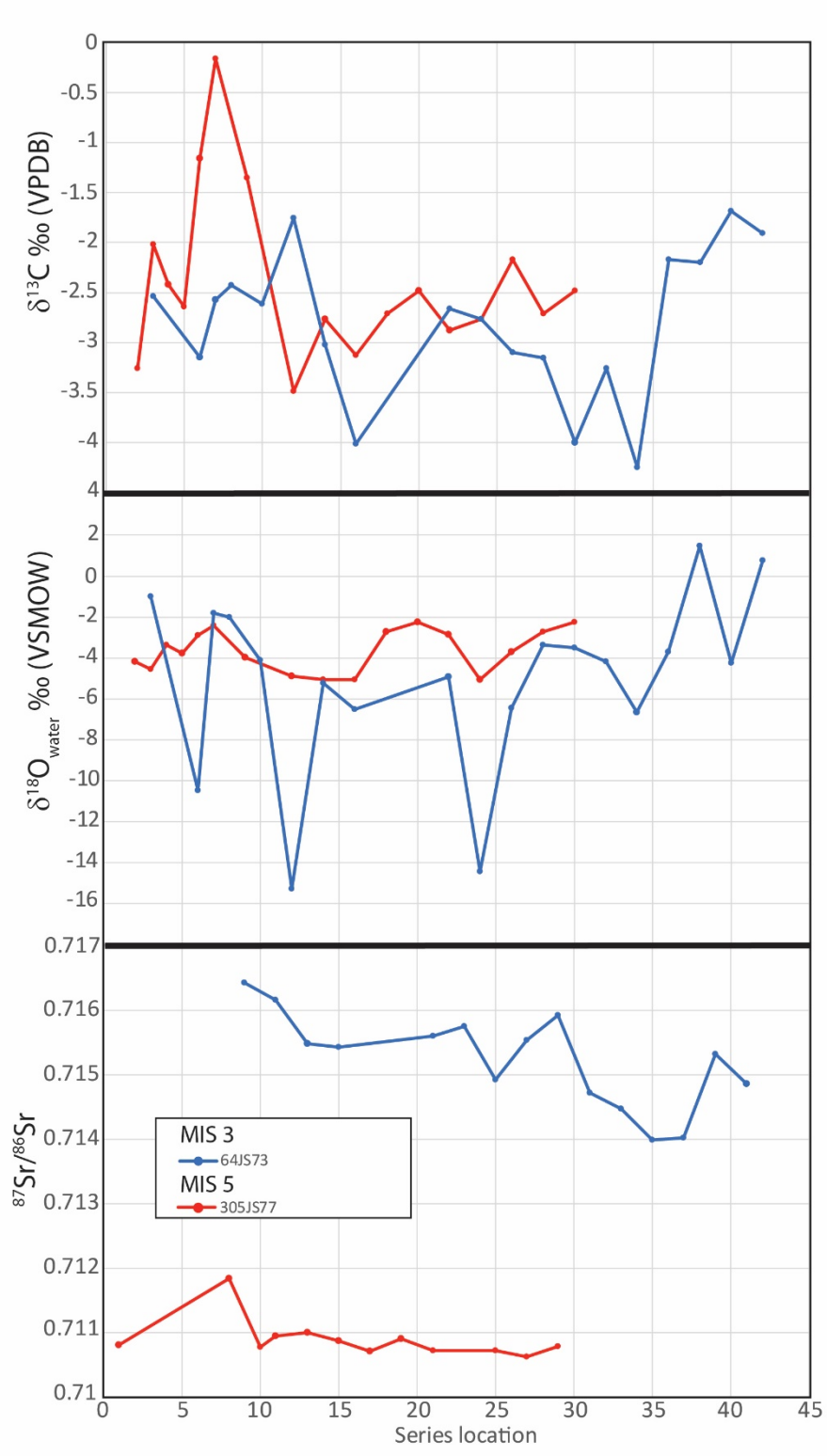

Figure 5. Time series, micro-sampled enamel $\delta^{13}C$, $\delta^{18}O$, $^{87}Sr/^{86}Sr$. Both specimens are from Jones Spring, Hickory County, Missouri.

328

329 The MIS 3 molar (64JS73) shows regular negative excursions in $\delta^{18}O$ values suggestive
330 of seasonal temperature changes in ingested water. These excursions are relatively short-lived
331 and extreme. Seasonal variation in enamel growth rate and maturation may account for the
332 perceived short length of these periods. Maximum $\delta^{18}O$ values in both mammoths are similar
333 however; the MIS 5e mammoth lacks these negative excursions and exhibits values that are more
334 complacent through the length of the tooth.

335 The $\delta^{13}C$ series from both molars indicate these mammoths experienced a C4 diet
336 throughout the year. However, deep dips in the $\delta^{18}O$ series of the MIS 3 molar also correspond to
337 at least two temporary peaks in the $\delta^{13}C$ series.

338 The $^{87}Sr/^{86}Sr$ isotope series from both animals demonstrate an adherence to separate
339 home ranges. The MIS 5e mammoth shows values similar to bedrock units outcropping locally
340 in central-western Missouri and neighboring areas of Kansas and Oklahoma. The MIS 3
341 mammoth, however, had a home range across rock units with much higher $^{87}Sr/^{86}Sr$ values. The
342 home ranges for these animals do not overlap, despite their recovery from different strata within
343 the same locality.

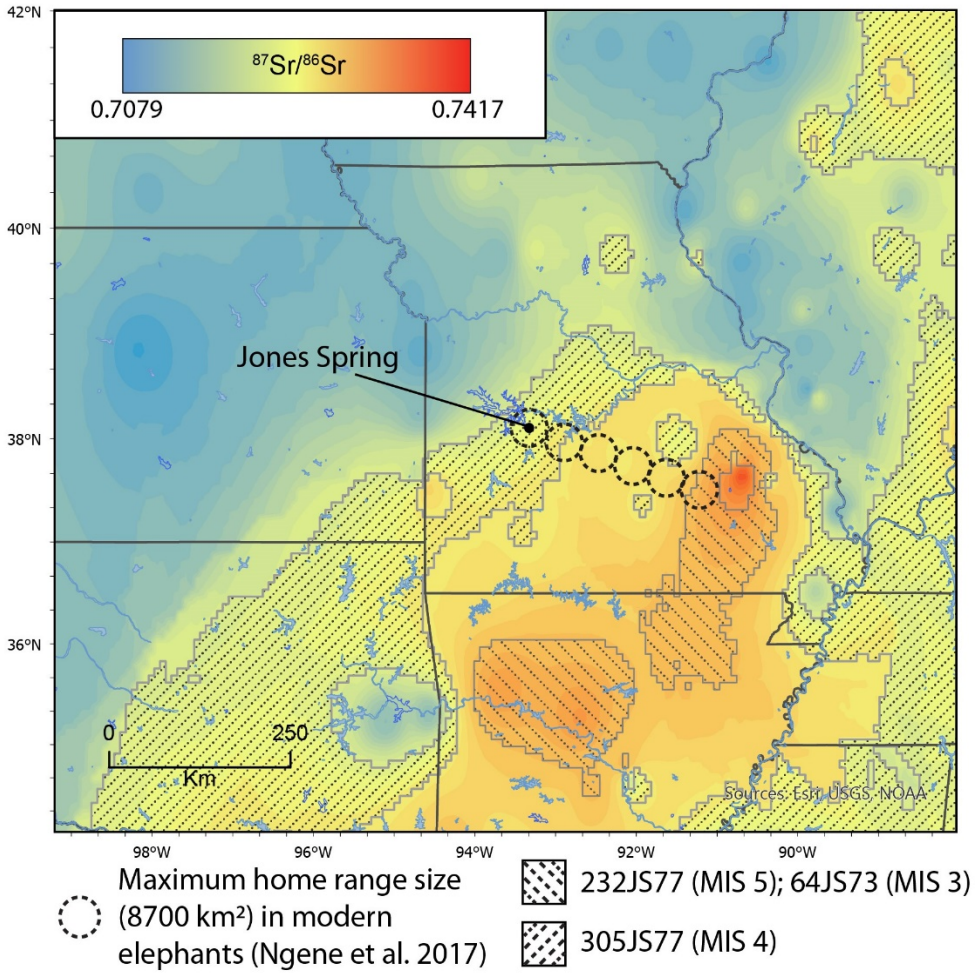

Figure 6. Mobility in mammoths from Jones Spring, Hickory Co., MO. Hatched areas indicate the range of $^{87}Sr/^{86}Sr$ values from mammoth molar ridge-plates. One mammoth (305JS77) exhibits local values. Two separate mammoths (232JS77, 64JS73) exhibit Sr values suggesting >200 km movement from the central core of the Ozark uplift. This implies movement over multiple years that is at least six times larger than the maximum home range size documented in modern elephants (Netosha National Park, Namibia). Basemap isoscape data from Widga et al. (2017b), Hedman et al. (2009, 2018).

DISCUSSION

Despite overall similar isotopic values in mammoths and mastodons throughout the period of this study, underlying nuances are informative to regional changes in niche structure and climate. The absence of mastodons during the coldest parts of the LGM suggests that *Mammut* were, at least to some degree, sensitive to colder climates and adjusted its range accordingly.

Comparisons between co-eval mammoths and mastodons indicate a gradual collapse of niche structure. Prior to MIS 2, $\delta^{13}C_{coll}$ and $\delta^{15}N_{coll}$ values between taxa were significantly different. By the end of the Allerød, mammoth and mastodon diets were isotopically indistinguishable.

Through time, there was no significant change in the $\delta^{13}C_{coll}$ of mastodons. Although average mammoth $\delta^{13}C_{coll}$ in the region during the latter part of the LGM was slightly more negative than other time periods, this is not a marked shift and may be a function of decreased pCO2 during that time (Schubert and Jahren 2015). Globally, Siberian and European mammoths exhibit a similar range of $\delta^{13}C_{coll}$ values (Iacumin et al. 2010; Szpak et al. 2010; Arppe et al. 2019; Schwartz-Narbonne et al. 2019).

In both taxa, mean $\delta^{15}N_{coll}$ decreases slightly throughout the sequence, however, the minimum $\delta^{15}N$ values for mastodons during the Bølling, Allerød, and Younger Dryas are significantly lower than earlier mastodons. The anomalously low values of these late mastodons are also shared with other published mastodon values in the Great Lakes region (Metcalfe et al. 2013). They are also significantly lower than contemporary midwestern, Eurasian or Beringean mammoths (with some exceptions, Drucker et al. 2018). The timing of these low, mastodon $\delta^{15}N_{coll}$ values correspond to regionally low $\delta^{15}N_{coll}$ values in the bone collagen of non-

375 proboscidean taxa from European late Quaternary contexts (Drucker et al., 2009; Richards and
376 Hedges, 2003; Rabanus-Wallace et al., 2017; Stevens et al., 2008) suggesting broad changes in
377 global climate may have had cascading impacts in the N budget of local ecosystems.

378 However, understanding in more detail how climate might have affected N cycling in
379 midwestern ecosystems remains unclear. Flux in soil and plant N may be a function of plant-
380 based N_2 fixation (Shearer and Kohl 1993), rooting depth (Schulze et al. 1994), N loss related to
381 climate factors (Austin and Vitousek 1998; Handley and Raven 1992), microbial activity, or
382 mycorrhizal colonization (Hobbie et al. 2000; Michelsen et al. 1998;). Furthermore, the role of
383 large herbivore populations in N flux may be significant (Frank et al. 2004). In N limited
384 environments such as tundra, terrestrial plants may receive relatively more N from inorganic
385 sources. Boreal forests like those of the Midwest during the Bølling and Allerød, however,
386 exhibit relatively greater biological productivity, so plant shoots are more likely to take in
387 volatized ammonia (low $\delta^{15}N$) from organic sources such as urea (Fujiyoshi et al. 2017).

388 At this time, it is difficult to distinguish which (if any) of these factors had an impact on
389 late Quaternary mastodon $\delta^{15}N_{coll}$ values. Although there is a wide range in $\delta^{15}N_{coll}$ of mammoths
390 and mastodons throughout the sequence, $\delta^{15}N_{coll}$ values below 5‰ are only present in mastodons
391 during post-LGM deglaciation in the lower Great Lakes (39-43 deg. latitude), throughout an area
392 suggested to be vegetated by a disharmonius flora dominated by Black Ash and Spruce
393 (Gonzales and Grimm 2009; Gill et al. 2009) (Figure 7). The low $\delta^{15}N_{coll}$ values suggest that
394 these mastodons occupied an undefined, local-scale, dietary niche that was not shared by
395 contemporary mammoths, or by earlier mastodons. Previous research has suggested that the
396 Bølling-Allerød may have been a time of high mastodon populations in the Great Lakes region
397 (Widga et al. 2017a). The concentration of mastodons around water sources may have had an

impact on the $\delta^{15}N$ of browsed plants due to increased contributions of herbivore urea. Isotopically light plant shoots can occur with increased utilization of volatized NH_4 from organic sources, including urea from herbivores.

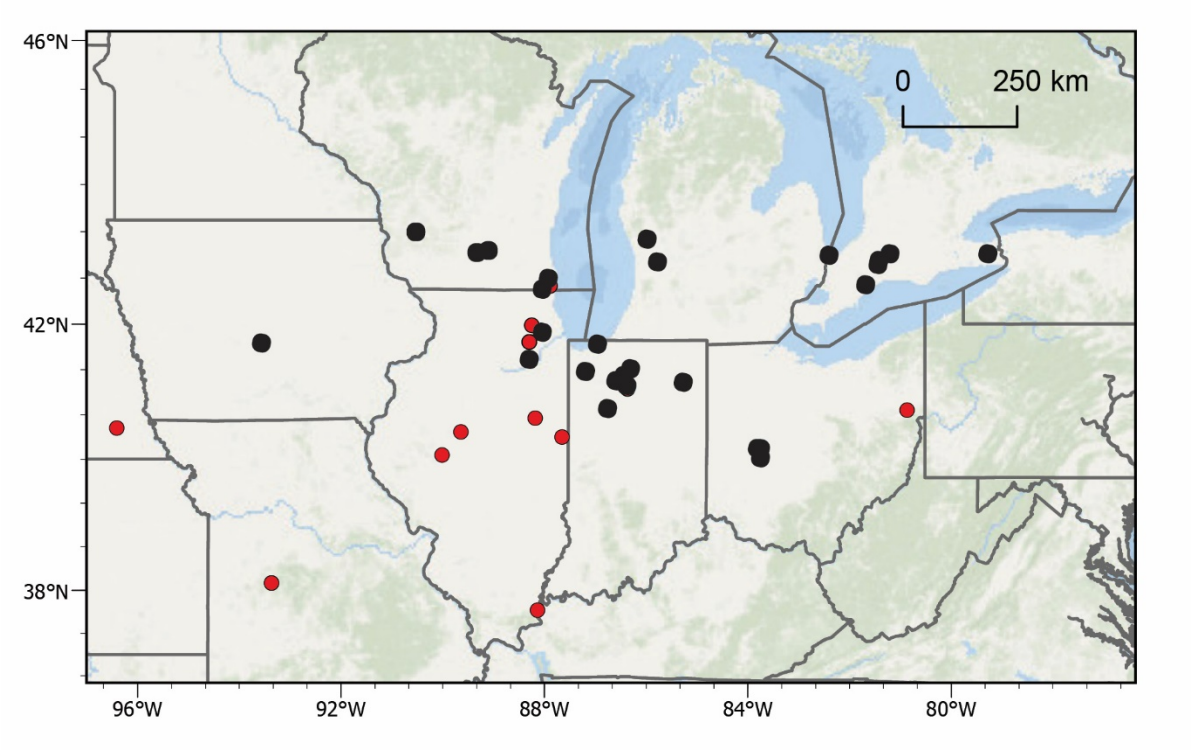

Figure 7. Mastodon distribution during the Bølling-Allerød. Black circles indicate mastodon $\delta^{15}N_{coll} < 5‰$. Red circles represent mastodons with $\delta^{15}N_{coll} > 5‰$.

Life Histories of midwestern Mammoths

Through analyses of incremental growth structures in mammoths, such as molar enamel or tusk dentin, we can reconstruct longitudinal life histories that reflect the landscape experienced by an animal over multiple years. Late Pleistocene mammoths from the study area exhibit relatively consistent, down-tooth patterns in $\delta^{13}C$ and $\delta^{18}O$. Similar bulk enamel isotope values in South Dakota, Wisconsin, and Illinois mammoths suggest access to broadly similar resources, and relatively stable access to these resources across multiple years of the life of an

412 individual (Figure 4). Less negative $\delta^{13}C$ and $\delta^{18}O$ values in the last forming samples of the
413 Schaeffer mammoth suggest a change in that animal's life history in the year before death. This
414 change could be explained by local environmental changes resulting in nutritional stress.
415 Two mammoths from the Jones Spring site in southwest Missouri provide a pre-LGM
416 perspective on landscapes that mammoths occupied (Figure 4). A tooth plate dating to MIS 5e
417 from Jones Spring has less negative $\delta^{18}O$ and $\delta^{13}C$ values compared to the MIS 2 samples. This
418 indicates warmer overall conditions and a diet that incorporated more C4 grasses throughout
419 multiple years. Pollen from the same stratigraphic units further suggest that southwestern
420 Missouri during MIS 5e was dominated by *Pinus* (no *Picea*) with a significant non-arboreal
421 component (King 1973). Importantly, Sr isotopes from this tooth indicate that while this tooth
422 was forming, the animal was foraging across surfaces that are more radiogenic than local values.
423 The nearest area with $^{87}Sr/^{86}Sr$ values >0.7140 is the central Ozark uplift to the east of Jones
424 Spring (Figure 6). The wide amplitude of $\delta^{18}O$ values throughout the length of this tooth,
425 combined with the Sr isotope data suggesting adherence to the central Ozark uplift suggest
426 relatively broad shifts in annual water availability and/or that this animal utilized a variety of
427 water sources, including surface sources and freshwater springs.
428 The MIS 4 molar from Jones Spring has $\delta^{18}O$ values intermediate between the MIS 2
429 samples and the MIS 5e sample, along with $\delta^{13}C$ values that indicate more C4 consumption than
430 MIS 2 samples (Figure 4). This mammoth occupied a cooler environment than the MIS 5e
431 mammoth, but significantly warmer than the late Pleistocene mammoths in the MIS 2 group.
432 In the case of the two, microsampled mammoths from Jones Spring, MO, isotopic trends
433 in each animal illustrates different life histories (Figure 5). The MIS 4 mammoth occupied the
434 western Ozarks as indicated by $^{87}Sr/^{86}Sr$ values deposited throughout the development of the

435 sampled portion of the tooth. It occupied a landscape where C4 vegetation was common, with
436 mild winter temperatures. The MIS 3 mammoth from Jones Spring occupied the central core of
437 the Ozark uplift indicated by $^{87}Sr/^{86}Sr$ values deposited during the formation of the sampled
438 tooth. However, between the cessation of enamel formation and death, this animal moved ~200
439 km to the western Ozarks where it was preserved in the Jones Spring deposits. The $\delta^{18}O$ series of
440 this animal suggests greater seasonality during MIS 3 compared to MIS 5e, with deep negative
441 excursions during the cold season. It also had a diet composed primarily of C4 vegetation.
442 These results suggest a broadly similar geographic scale of landscape-use in late
443 Quaternary mammoths in the Midwest to mammoths in the Great Plains and Florida (Esker et al.
444 2019; Hoppe et al. 1999; Hoppe 2004). Overall, mammoths from both regions do not engage in
445 significant seasonal migrations, but can move greater distances at annual to decadal time-scales.
446 Further, although $\delta^{13}C_{coll}$ values in mammoths clearly suggest a niche that, at times, included C3-
447 rich diets in a region that was dominated by forest, not grasslands, both Jones Spring mammoths
448 were mixed feeders with C4 grasses making up a significant part of their diet. The individual life
449 histories of these mammoths are highly variable, underscoring the need to control for individual
450 mobility in stable isotope studies of large herbivore taxa.
451 Testing scenarios of late Pleistocene Proboscidean population dynamics
452 Can this stable isotope dataset illuminate trends in late Proboscidean population
453 dynamics during deglaciation in the Midwest? It is possible that the shift in $\delta^{15}N$ represents the
454 colonization of a novel ecological niche that also coincides with climate and vegetational
455 changes at the beginning of the Bølling-Allerød. However, it is unclear what this niche might be.
456 Stable isotopes alone do not adequately define this niche space, and further paleobotanical work
457 is necessary. Drucker et al. (2018) also noted anomalously low $\delta^{15}N$ values in LGM mammoths

458 from Mezyhrich in central Europe, and attributed this pattern to a large, but unspecific, shift in
459 dietary niche. This is counter-intuitive in warming landscapes of the Midwest since boreal forests
460 typically have increased amounts of N fixing microbes relative to tundra environments, thus
461 increasing the $\delta^{15}N$ in forage, overall.

462 Some studies have suggested that the growth rate of an individual is inversely correlated
463 with $\delta^{15}N$ (Warinner and Tuross 2010). This would be consistent with some scenarios of late
464 Pleistocene mastodon population dynamics. Fisher (Fisher 2009; 2018) suggests that predator
465 pressure from Paleoindian groups who were megafaunal specialists would have caused
466 mastodons to mature at a younger age. A decrease in the age at weaning would mean a shorter
467 period of nursing-related, elevated dietary $\delta^{15}N$ in young mastodons. If this were the case, we
468 would expect an overall decrease in $\delta^{15}N$ of bone collagen in animals in their first and second
469 decade of life. In our dataset, there is no significant change in maximum or mean $\delta^{15}N$ in
470 mastodon bone collagen, despite a subset of mastodons that have lower $\delta^{15}N$ values. If predator
471 pressure is contributing to faster maturation and shortening the time of nursing, then it is only
472 occurring in some areas. However, even if this were the case in these areas, it is still uncertain
473 what ecological processes might drive an increase in growth rate. Depending on local forage
474 conditions experienced by an animal, an increase in growth rate may be caused by increased
475 predator pressure (Fisher 2009) or a decrease in population density (Wolverton et al. 2009).

476 It is also possible that low $\delta^{15}N$ values in post-LGM mastodons represents a systematic
477 change in predator avoidance strategies among some mastodon populations (Fiedel et al. 2019).
478 Mastodons may have been attracted to low $\delta^{15}N$ areas such as marshes and wetlands as a
479 response to new predators on the landscape (i.e., humans). However, taphonomic modification of
480 late Pleistocene proboscidean materials by humans or other predators is extremely rare in this

dataset (Widga et al. 2017a), so we see this scenario as an unlikely driver of mastodon landscape use.

If proboscidean populations are dense on the landscape (Widga et al. 2017a) there may also be rapid, significant, and long-term changes to N cycle. An influx of N via urea as would be expected in high-density areas, would cause isotopically heavy plant roots and isotopically light shoots. Under intense grazing pressure, changes to N contributions change quickly from inorganic soil mineral N reservoirs to N from urea (McNaughton et al. 1988; Knapp et al. 1999). Individuals with lower $\delta^{15}N_{coll}$ values during the Allerød lived in areas with high mastodon populations, which may have contributed to isotopically light forage (due to ammonia volitization, Knapp et al. 1999). However, this scenario does not explain why this shift is absent in mammoths during this time.

CONCLUSIONS

Stable isotopes of proboscidean tissues in the midwestern US illustrate the variability inherent in modern paleoecological analyses. Traditional approaches to understanding animal diets and landscape use through morphology and a reliance on modern analogues is inadequate for understanding paleoecological changes within megafaunal populations, or during times of rapid ecological change such as the late Quaternary.

Stable isotopes from bone collagen of midwestern proboscideans suggest consistently C3-dominated diets over the last 50 ka. During the LGM, mammoth diets may have included C3 grasses, but the prevalence of C3 flora during the post-LGM period is likely due to a landscape

shift to more forest (Gonzales and Grimm 2009; Saunders et al. 2010) with grasses making up very little of the floral communities in the southern Great Lakes region.

Despite the strong C3-signal in mammoth and mastodon diets during this period, the range of dietary flexibility and the degree of overlap between these two taxa is striking. The isotopically defined dietary niche of mammoths and mastodons show increasing overlap as they approach extinction. Niche overlap is also supported by assemblages where both taxa co-occur (Saunders et al. 2010; Widga et al. 2017a). However, there are exceptions to this pattern and some late mastodons exhibit low $\delta^{15}N$ values that may indicate the evolution and occupation of a new dietary niche, physiological responses to late Pleistocene ecological changes, or some other process acting on late mastodon populations.

Further resolution of mammoth and mastodon life histories are gleaned from stable isotopes in tooth enamel. $\delta^{13}C$ and $\delta^{18}O$ generally track climate and landscape changes experienced during tooth formation. MIS 2 mammoths are broadly similar in their isotopic life histories and illustrate relative homogeneity of landscape conditions across the Midwest at this time. Micro-sampled mammoth molars from Jones Spring, MO, indicate a significant increase in MIS 3 seasonality, compared to the last interglacial period (MIS 5e). Finally, some mammoths in this study died >200 km away from where they lived during the formation of sampled molars suggesting lifetime mobility patterns in mammoths could have a significant effect on presumed 'local' stable isotope values.

Acknowledgements.

523 The study benefited from discussions with Paul Countryman, Eric Grimm, and Bonnie
524 Styles, then at the Illinois State Museum; Rhiannon Stevens (University College of London) and
525 Matt G. Hill (Iowa State University). Additional conversations with Don Esker greatly clarified
526 micro-milling methods, and Joseph Andrew (University of Kansas) assisted with Sr isotope
527 analyses. Jeff Pigati and two anonymous reviewers provided invaluable feedback for
528 strengthening the manuscript. This research was funded by NSF grants 1050638, 1049885 and
529 1050261 and the Illinois State Museum Society. Finally, we would like to acknowledge all of the
530 collections managers and curators who assisted us with access to the specimens within their care.
531
532

533 **Figures**

534 Figure 1. Map of dated midwestern mammoths (blue) and mastodons (red) with

535 associated $\delta^{13}C_{coll}$ and $\delta^{15}N_{coll}$ data. See SM Table 2 for details.

536 Figure 2. Schematic illustration of serial and micro-sampling strategies.

537 Figure 3. Changes in midwestern proboscidean collagen $\delta^{13}C$ and $\delta^{15}N$ through time.

538 Figure 4. Time series, serial enamel $\delta^{13}C$, $\delta^{18}O$, $^{87}Sr/^{86}Sr$.

539 Figure 5. Time series, micro-sampled enamel $\delta^{13}C$, $\delta^{18}O$, $^{87}Sr/^{86}Sr$. Both specimens are

540 from Jones Spring, Hickory County, Missouri.

541 Figure 6. Mobility in mammoths from Jones Spring, Hickory Co., MO. Hatched areas

542 indicate the range of $^{87}Sr/^{86}Sr$ values from mammoth molar ridge-plates. One mammoth

543 (305JS77) exhibits local values. Two separate mammoths (232JS77, 64JS73) exhibit Sr

544 values suggesting >200 km movement from the central core of the Ozark uplift. This

545 implies movement over multiple years that is at least six times larger than the maximum

546 home range size documented in modern elephants (Netosha National Park, Namibia).

547 Basemap isoscape data from Widga et al. (2017b), Hedman et al. (2009, 2018).

548 Figure 7. Mastodon distribution during the Bølling-Allerød. Black circles indicate

549 mastodon $\delta^{15}N_{coll} < 5‰$. Red circles represent mastodons with $\delta^{15}N_{coll} > 5‰$.

550

551 **Tables**

552 Table 1. Temporal Scale in Paleoecological Analyses.

553 Table 2. Mammoth and mastodon collagen stable isotope values, by chronzone.

554 Table 3. Summary of serial and micro-sampled tooth enamel series: $\delta^{13}C$, $\delta^{18}O$, $^{87}Sr/^{86}Sr$.

555

Supplemental information

SM Supplemental Material. Word File

SM Table 1. Mammoth and Mastodon $\delta^{13}C$, $\delta^{15}N$ data.

SM Table 2. Mammoth enamel isotope data.

SM Table 3. Radiocarbon dated mammoths and mastodons from the Midwest.

References

Alley, Richard B. 2000. "The Younger Dryas Cold Interval as Viewed from Central Greenland." *Quaternary Science Reviews* 19 (1): 213–26. https://doi.org/10.1016/S0277-3791(99)00062-1.

Alroy, John. 2001. "A Multispecies Overkill Simulation of the End-Pleistocene Megafaunal Mass Extinction." *Science* 292 (5523): 1893–96. https://doi.org/10.1126/science.1059342.

Arppe, Laura, Juha A. Karhu, Sergey Vartanyan, Dorothée G. Drucker, Heli Etu-Sihvola, and Hervé Bocherens. 2019. "Thriving or Surviving? The Isotopic Record of the Wrangel Island Woolly Mammoth Population." *Quaternary Science Reviews* 222 (October): 105884. https://doi.org/10.1016/j.quascirev.2019.105884.

Augustine, David J., Samuel J. McNaughton, and Douglas A. Frank. 2003. "Feedbacks Between Soil Nutrients and Large Herbivores in a Managed Savanna Ecosystem." *Ecological Applications* 13 (5): 1325–37. https://doi.org/10.1890/02-5283.

Austin, Amy T., and P. M. Vitousek. 1998. "Nutrient Dynamics on a Precipitation Gradient in Hawai'i." *Oecologia* 113 (4): 519–29. https://doi.org/10.1007/s004420050405.

Bataille, Clément P., and Gabriel J. Bowen. 2012. "Mapping 87Sr/86Sr Variations in Bedrock and Water for Large Scale Provenance Studies." *Chemical Geology* 304–305 (April): 39–52. https://doi.org/10.1016/j.chemgeo.2012.01.028.

Baumann, Eric J., and Brooke E. Crowley. 2015. "Stable Isotopes Reveal Ecological Differences amongst Now-Extinct Proboscideans from the Cincinnati Region, USA." *Boreas* 44 (1): 240–54. https://doi.org/10.1111/bor.12091.

Birks, Hilary H., Bas van Geel, Daniel C. Fisher, Eric C. Grimm, Wim J. Kuijper, Jan van Arkel, and Guido B. A. van Reenen. 2019. "Evidence for the Diet and Habitat of Two Late Pleistocene Mastodons from the Midwest, USA." *Quaternary Research* 91 (2): 792–812. https://doi.org/10.1017/qua.2018.100.

Bocherens, Hervé, Gilles Pacaud, Petr A. Lazarev, and André Mariotti. 1996. "Stable Isotope Abundances (13C, 15N) in Collagen and Soft Tissues from Pleistocene Mammals from Yakutia: Implications for the Palaeobiology of the Mammoth Steppe." *Palaeogeography, Palaeoclimatology, Palaeoecology*, Biogenic Phosphates as Palaeoenvironmental Indicators, 126 (1): 31–44. https://doi.org/10.1016/S0031-0182(96)00068-5.

Brock, Fiona, Thomas Higham, Peter Ditchfield, and Christopher Bronk Ramsey. 2010. "Current Pretreatment Methods for AMS Radiocarbon Dating at the Oxford Radiocarbon

Accelerator Unit (Orau).” *Radiocarbon* 52 (1): 103–12. https://doi.org/10.1017/S0033822200045069.

Broughton, Jack M., and Elic M. Weitzel. 2018. “Population Reconstructions for Humans and Megafauna Suggest Mixed Causes for North American Pleistocene Extinctions.” *Nature Communications* 9 (1): 5441. https://doi.org/10.1038/s41467-018-07897-1.

Cerling, Thure E., George Wittemyer, James R. Ehleringer, Christopher H. Remien, and Iain Douglas-Hamilton. 2009. “History of Animals Using Isotope Records (HAIR): A 6-Year Dietary History of One Family of African Elephants.” *Proceedings of the National Academy of Sciences* 106 (20): 8093–8100. https://doi.org/10.1073/pnas.0902192106.

Chafota, Jonas, and Norman Owen-Smith. 2009. “Episodic Severe Damage to Canopy Trees by Elephants: Interactions with Fire, Frost and Rain.” *Journal of Tropical Ecology* 25 (3): 341–45. https://doi.org/10.1017/S0266467409006051.

Coe, Malcolm. 1978. “The Decomposition of Elephant Carcases in the Tsavo (East) National Park, Kenya.” *Journal of Arid Environments* 1 (1): 71–86. https://doi.org/10.1016/S0140-1963(18)31756-7.

Coltrain, Joan Brenner, John M. Harris, Thure E. Cerling, James R. Ehleringer, Maria-Denise Dearing, Joy Ward, and Julie Allen. 2004. “Rancho La Brea Stable Isotope Biogeochemistry and Its Implications for the Palaeoecology of Late Pleistocene, Coastal Southern California.” *Palaeogeography, Palaeoclimatology, Palaeoecology* 205 (3): 199–219. https://doi.org/10.1016/j.palaeo.2003.12.008.

Daniel Bryant, J., and Philip N. Froelich. 1995. “A Model of Oxygen Isotope Fractionation in Body Water of Large Mammals.” *Geochimica et Cosmochimica Acta* 59 (21): 4523–4537. https://doi.org/10.1016/0016-7037(95)00250-4.

Daux, Valérie, Christophe Lécuyer, Marie Anne Héran, Romain Amiot, Laurent Simon, François Fourel, François Martineau, Niels Lynnerup, Hervé Reychler, and Gilles Escarguel. 2008. “Oxygen Isotope Fractionation between Human Phosphate and Water Revisited.” *Journal of Human Evolution* 55 (6): 1138–1147. https://doi.org/10.1016/j.jhevol.2008.06.006.

Davis, Matt, and Silvia Pineda-Munoz. 2016. “The Temporal Scale of Diet and Dietary Proxies.” *Ecology and Evolution* 6 (6): 1883–97. https://doi.org/10.1002/ece3.2054.

Delcourt, Hazel R., and P. Delcourt. 1991. *Quaternary Ecology: A Paleoecological Perspective*. Springer Science & Business Media.

Denny, Mark W., Brian Helmuth, George H. Leonard, Christopher D. G. Harley, Luke J. H. Hunt, and Elizabeth K. Nelson. 2004. “Quantifying scale in ecology: lessons from a wave-swept shore.” *Ecological Monographs* 74 (3): 513–32. https://doi.org/10.1890/03-4043.

Dirks, Wendy, Timothy G. Bromage, and Larry D. Agenbroad. 2012. “The Duration and Rate of Molar Plate Formation in Palaeoloxodon Cypriotes and Mammuthus Columbi from Dental Histology.” *Quaternary International*, Mammoths and Their Relatives 1: Biotopes, Evolution and Human Impact V International Conference, Le Puy-en-Velay, 2010, 255 (March): 79–85. https://doi.org/10.1016/j.quaint.2011.11.002.

Drucker, D. G., Bridault, A., Iacumin, P., & Bocherens, H. (2009). Bone stable isotopic signatures (15N, 18O) as tracers of temperature variation during the Late-glacial and early Holocene: case study on red deer *Cervus elaphus* from Rochedane (Jura, France). *Geological Journal*, 44(5), 593-604.

Drucker, Dorothée G., Rhiannon E. Stevens, Mietje Germonpré, Mikhail V. Sablin, Stéphane Péan, and Hervé Bocherens. 2018. “Collagen Stable Isotopes Provide Insights into the

642 End of the Mammoth Steppe in the Central East European Plains during the
643 Epigravettian." *Quaternary Research* 90 (3): 457–69.
644 https://doi.org/10.1017/qua.2018.40.
645 El Adli, Joseph J., Michael D. Cherney, Daniel C. Fisher, John M. Harris, Farrell, Aisling, and
646 Cox, Shelley. 2015. "Last Years of Life and Season of Death of a Columbian Mammoth
647 from Rancho La Brea." *Science Series, Natural History Museum of Los Angeles County*
648 42: 65–80.
649 El Adli, Joseph J., Daniel C. Fisher, Sergey L. Vartanyan, and Alexei N. Tikhonov. 2017. "Final
650 Years of Life and Seasons of Death of Woolly Mammoths from Wrangel Island and
651 Mainland Chukotka, Russian Federation." *Quaternary International*, VIth International
652 Conference on Mammoths and their Relatives, Part 3, 445 (July): 135–45.
653 https://doi.org/10.1016/j.quaint.2016.07.017.
654 Esker, D., Forman, S. L., Widga, C., Walker, J. D., & Andrew, J. E. (2019). Home range of the
655 Columbian mammoths (*Mammuthus columbi*) and grazing herbivores from the Waco
656 Mammoth National Monument,(Texas, USA) based on strontium isotope ratios from
657 tooth enamel bioapatite. *Palaeogeography, Palaeoclimatology, Palaeoecology*, 534,
658 109291.
659 Fiedel, Stuart, Robert Feranec, Thomas Marino, and David Driver. 2019. "A New AMS
660 Radiocarbon Date for the Ivory Pond Mastodon." *Eastern Paleontologist* 3: 1–15.
661 Fisher, Daniel C. 2009. "Paleobiology and Extinction of Proboscideans in the Great Lakes
662 Region of North America." In *American Megafaunal Extinctions at the End of the*
663 *Pleistocene*, edited by Gary Haynes, 55–75. Vertebrate Paleobiology and
664 Paleoanthropology. Dordrecht: Springer Netherlands. https://doi.org/10.1007/978-1-
665 4020-8793-6_4.
666 ———. 2018. "Paleobiology of Pleistocene Proboscideans." *Annual Review of Earth and*
667 *Planetary Sciences* 46 (1): 229–60. https://doi.org/10.1146/annurev-earth-060115-
668 012437.
669 Fisher, Daniel C., and David L. Fox. 2006. "Five Years in the Life of an Aucilla River
670 Mastodon." In *First Floridians and Last Mastodons: The Page-Ladson Site in the Aucilla*
671 *River*, edited by S. David Webb, 343–77. Dordrecht: Springer Netherlands.
672 https://doi.org/10.1007/978-1-4020-4694-0_12.
673 Fisher, Daniel C., Alexei N. Tikhonov, Pavel A. Kosintsev, Adam N. Rountrey, Bernard
674 Buigues, and Johannes van der Plicht. 2012. "Anatomy, Death, and Preservation of a
675 Woolly Mammoth (Mammuthus Primigenius) Calf, Yamal Peninsula, Northwest
676 Siberia." *Quaternary International*, Mammoths and Their Relatives 1: Biotopes,
677 Evolution and Human Impact V International Conference, Le Puy-en-Velay, 2010, 255
678 (March): 94–105. https://doi.org/10.1016/j.quaint.2011.05.040.
679 Fortelius, Mikael, and Nikos Solounias. 2000. "Functional Characterization of Ungulate Molars
680 Using the Abrasion-Attrition Wear Gradient: A New Method for Reconstructing
681 Paleodiets." *American Museum Novitates* 225 (4): 1–36. https://doi.org/10.1206/0003-
682 0082(2000)301<0001:FCOUMU>2.0.CO;2.
683 Fox, David L., and Daniel C. Fisher. 2001. "Stable Isotope Ecology of a Late Miocene
684 Population of Gomphotherium Productus (Mammalia, Proboscidea) from Port of Entry
685 Pit, Oklahoma, USA." *PALAIOS* 16 (3): 279–93. https://doi.org/10.1669/0883-
686 1351(2001)016<0279:SIEOAL>2.0.CO;2.
687 Fox-Dobbs, K., J.K. Bump, R.O. Peterson, D.L. Fox, and P.L. Koch. 2007. "Carnivore-Specific

688 Stable Isotope Variables and Variation in the Foraging Ecology of Modern and Ancient
689 Wolf Populations: Case Studies from Isle Royale, Minnesota, and La Brea." *Canadian*
690 *Journal of Zoology* 85 (4): 458–71. https://doi.org/10.1139/Z07-018.
691 Fox-Dobbs, Kena, Jennifer A. Leonard, and Paul L. Koch. 2008. "Pleistocene Megafauna from
692 Eastern Beringia: Paleoecological and Paleoenvironmental Interpretations of Stable
693 Carbon and Nitrogen Isotope and Radiocarbon Records." *Palaeogeography,*
694 *Palaeoclimatology, Palaeoecology* 261 (1): 30–46.
695 https://doi.org/10.1016/j.palaeo.2007.12.011.
696 Frank, Douglas A., R. David Evans, and Benjamin F. Tracy. 2004. "The Role of Ammonia
697 Volatilization in Controlling the Natural ^{15} N Abundance of a Grazed Grassland."
698 *Biogeochemistry* 68 (2): 169–78. https://doi.org/10.1023/B:BIOG.0000025736.19381.91.
699 Fujiyoshi, Lei, Atsuko Sugimoto, Akemi Tsukuura, Asami Kitayama, M. Larry Lopez Caceres,
700 Byambasuren Mijidsuren, Ariunaa Saraadanbazar, and Maki Tsujimura. 2017. "Spatial
701 Variations in Larch Needle and Soil δ^{15} N at a Forest–Grassland Boundary in Northern
702 Mongolia." *Isotopes in Environmental and Health Studies* 53 (1): 54–69.
703 https://doi.org/10.1080/10256016.2016.1206093.
704 Geel, Bas van, Daniel C. Fisher, Adam N. Rountrey, Jan van Arkel, Joost F. Duivenvoorden,
705 Aline M. Nieman, Guido B. A. van Reenen, Alexei N. Tikhonov, Bernard Buigues, and
706 Barbara Gravendeel. 2011. "Palaeo-Environmental and Dietary Analysis of Intestinal
707 Contents of a Mammoth Calf (Yamal Peninsula, Northwest Siberia)." *Quaternary*
708 *Science Reviews* 30 (27): 3935–46. https://doi.org/10.1016/j.quascirev.2011.10.009.
709 Gill, Jacquelyn L., John W. Williams, Stephen T. Jackson, Katherine B. Lininger, and Guy S.
710 Robinson. 2009. "Pleistocene Megafaunal Collapse, Novel Plant Communities, and
711 Enhanced Fire Regimes in North America." *Science* 326 (5956): 1100–1103.
712 https://doi.org/10.1126/science.1179504.
713 Gonzales, Leila M., and Eric C. Grimm. 2009. "Synchronization of Late-Glacial Vegetation
714 Changes at Crystal Lake, Illinois, USA with the North Atlantic Event Stratigraphy."
715 *Quaternary Research* 72 (2): 234–45. https://doi.org/10.1016/j.yqres.2009.05.001.
716 Gonzales, L.M., J.W. Williams, and E.C. Grimm. 2009. "Expanded Response-Surfaces: A New
717 Method to Reconstruct Paleoclimates from Fossil Pollen Assemblages That Lack Modern
718 Analogues." *Quaternary Science Reviews* 28 (27–28): 3315–32.
719 https://doi.org/10.1016/j.quascirev.2009.09.005.
720 Green, Jeremy L., Larisa R. G. DeSantis, and Gregory James Smith. 2017. "Regional Variation
721 in the Browsing Diet of Pleistocene Mammut Americanum (Mammalia, Proboscidea) as
722 Recorded by Dental Microwear Textures." *Palaeogeography, Palaeoclimatology,*
723 *Palaeoecology* 487 (December): 59–70. https://doi.org/10.1016/j.palaeo.2017.08.019.
724 Guldemond, Robert, and Rudi Van Aarde. 2008. "A Meta-Analysis of the Impact of African
725 Elephants on Savanna Vegetation." *The Journal of Wildlife Management* 72 (4): 892–99.
726 Handley, L. L., and J. A. Raven. 1992. "The Use of Natural Abundance of Nitrogen Isotopes in
727 Plant Physiology and Ecology." *Plant, Cell and Environment* 15 (9): 965–85.
728 https://doi.org/10.1111/j.1365-3040.1992.tb01650.x.
729 Hedges, Robert E. M., John G. Clement, C. David L. Thomas, and Tamsin C. O'Connell. 2007.
730 "Collagen Turnover in the Adult Femoral Mid-Shaft: Modeled from Anthropogenic
731 Radiocarbon Tracer Measurements." *American Journal of Physical Anthropology* 133
732 (2): 808–16. https://doi.org/10.1002/ajpa.20598.
733 Hedman, Kristin M., B. Brandon Curry, Thomas M. Johnson, Paul D. Fullagar, and Thomas E.

734 Emerson. 2009. "Variation in Strontium Isotope Ratios of Archaeological Fauna in the
735 Midwestern United States: A Preliminary Study." *Journal of Archaeological Science* 36
736 (1): 64–73. https://doi.org/10.1016/j.jas.2008.07.009.
737 Hedman, Kristin M., Philip A. Slater, Matthew A. Fort, Thomas E. Emerson, and John M.
738 Lambert. 2018. "Expanding the Strontium Isoscape for the American Midcontinent:
739 Identifying Potential Places of Origin for Cahokian and Pre-Columbian Migrants."
740 *Journal of Archaeological Science: Reports* 22 (September): 202–213.
741 https://doi.org/10.1016/j.jasrep.2018.09.027.
742 Higham, T F G, R M Jacobi, and C B Ramsey. 2006. "AMS Radiocarbon Dating of Ancient
743 Bone Using Ultrafiltration." *Radiocarbon* 48 (2): 179–195.
744 https://doi.org/10.2458/azu_js_rc.v48i2.2861.
745 Hobbie, E. A., S. A. Macko, and M. Williams. 2000. "Correlations between Foliar Δ15N and
746 Nitrogen Concentrations May Indicate Plant-Mycorrhizal Interactions." *Oecologia* 122
747 (2): 273–83. https://doi.org/10.1007/PL00008856.
748 Hoppe, Kathryn A. 2004. "Late Pleistocene Mammoth Herd Structure, Migration Patterns, and
749 Clovis Hunting Strategies Inferred from Isotopic Analyses of Multiple Death
750 Assemblages." *Paleobiology* 30 (1): 129–45. https://doi.org/10.1666/0094-
751 8373(2004)030<0129:LPMHSM>2.0.CO;2.
752 Hoppe, Kathryn A., and Paul L. Koch. 2007. "Reconstructing the Migration Patterns of Late
753 Pleistocene Mammals from Northern Florida, USA." *Quaternary Research* 68 (3): 347–
754 52. https://doi.org/10.1016/j.yqres.2007.08.001.
755 Hoppe, Kathryn A., Paul L. Koch, Richard W. Carlson, and S. David Webb. 1999. "Tracking
756 Mammoths and Mastodons: Reconstruction of Migratory Behavior Using Strontium
757 Isotope Ratios." *Geology* 27 (5): 439–42. https://doi.org/10.1130/0091-
758 7613(1999)027<0439:TMAMRO>2.3.CO;2.
759 Iacumin, P., A. Di Matteo, V. Nikolaev, and T. V. Kuznetsova. 2010. "Climate Information from
760 C, N and O Stable Isotope Analyses of Mammoth Bones from Northern Siberia."
761 *Quaternary International*, Quaternary Changes of Mammalian Communities Across and
762 Between Continents, 212 (2): 206–12. https://doi.org/10.1016/j.quaint.2009.10.009.
763 Keenan, Sarah W., Chris Widga, Debruyn, Jennifer, and schaeffer, sean. 2018. "Nutrient
764 Hotspots through Time: A Field Guide to Modern and Fossil Taphonomy in East
765 Tennessee." In *Geology at Every Scale*, by Annette Summers Engel and Robert D.
766 Hatcher, 61–74. Geological Society of America. https://doi.org/10.1130/2018.0050(04).
767 King, J. E. (1973). Late Pleistocene palynology and biogeography of the western Missouri
768 Ozarks. Ecological Monographs, 43(4): 539-565.
769 Knapp, Alan K, John M Blair, John M Briggs, Scott L Collins, David C Hartnett, Loretta C
770 Johnson, E Gene Towne, M John, and L Scott. 1999. "North Keystone Role of Bison in
771 American Tallgrass Prairie Bison Increase Habitat Heterogeneity and Alter a Broad
772 Array of Processes" 49 (1): 39–50.
773 Koch, Paul L., Kathryn A. Hoppe, and S. David Webb. 1998. "The Isotopic Ecology of Late
774 Pleistocene Mammals in North America: Part 1. Florida." *Chemical Geology* 152 (1):
775 119–38. https://doi.org/10.1016/S0009-2541(98)00101-6.
776 Koch, Paul L., Noreen Tuross, and Marilyn L. Fogel. 1997. "The Effects of Sample Treatment
777 and Diagenesis on the Isotopic Integrity of Carbonate in Biogenic Hydroxylapatite."
778 *Journal of Archaeological Science* 24 (5): 417–429.
779 https://doi.org/10.1006/jasc.1996.0126.

780 Lee-Thorp, Julia, and Matt Sponheimer. 2003. "Three Case Studies Used to Reassess the
781 Reliability of Fossil Bone and Enamel Isotope Signals for Paleodietary Studies." *Journal*
782 *of Anthropological Archaeology* 22 (3): 208–216. https://doi.org/10.1016/S0278-
783 4165(03)00035-7.
784 Lepper, Bradley T., Tod A. Frolking, Daniel C. Fisher, Gerald Goldstein, Jon E. Sanger, Dee
785 Anne Wymer, J. Gordon Ogden, and Paul E. Hooge. 1991. "Intestinal Contents of a Late
786 Pleistocene Mastodont from Midcontinental North America." *Quaternary Research* 36
787 (1): 120–25. https://doi.org/10.1016/0033-5894(91)90020-6.
788 McNaughton, S. J., R. W. Ruess, and S. W. Seagle. 1988. "Large Mammals and Process
789 Dynamics in African Ecosystems." *BioScience* 38 (11): 794–800.
790 https://doi.org/10.2307/1310789.
791 Metcalfe, Jessica Z., and Fred J. Longstaffe. 2012. "Mammoth Tooth Enamel Growth Rates
792 Inferred from Stable Isotope Analysis and Histology." *Quaternary Research* 77 (3): 424–
793 32. https://doi.org/10.1016/j.yqres.2012.02.002.
794 ———. 2014. "Environmental Change and Seasonal Behavior of Mastodons in the Great Lakes
795 Region Inferred from Stable Isotope Analysis." *Quaternary Research* 82 (2): 366–77.
796 https://doi.org/10.1016/j.yqres.2014.07.002.
797 Metcalfe, Jessica Z., Fred J. Longstaffe, Jesse A. M. Ballenger, and C. Vance Haynes. 2011.
798 "Isotopic Paleoecology of Clovis Mammoths from Arizona." *Proceedings of the National*
799 *Academy of Sciences* 108 (44): 17916–20. https://doi.org/10.1073/pnas.1113881108.
800 Metcalfe, Jessica Z., Fred J. Longstaffe, and Greg Hodgins. 2013. "Proboscideans and
801 Paleoenvironments of the Pleistocene Great Lakes: Landscape, Vegetation, and Stable
802 Isotopes." *Quaternary Science Reviews* 76 (September): 102–13.
803 https://doi.org/10.1016/j.quascirev.2013.07.004.
804 Michelsen, Anders, Chris Quarmby, Darren Sleep, and Sven Jonasson. 1998. "Vascular Plant 15
805 N Natural Abundance in Heath and Forest Tundra Ecosystems Is Closely Correlated with
806 Presence and Type of Mycorrhizal Fungi in Roots." *Oecologia* 115 (3): 406–18.
807 https://doi.org/10.1007/s004420050535.
808 Mosimann, James E., and Paul S. Martin. 1975. "Simulating Overkill by Paleoindians: Did Man
809 Hunt the Giant Mammals of the New World to Extinction? Mathematical Models Show
810 That the Hypothesis Is Feasible." *American Scientist* 63 (3): 304–13.
811 Newsom, Lee A., and Mathew C. Mihlbachler. 2006. "Mastodons (Mammut Americanum) Diet
812 Foraging Patterns Based on Analysis of Dung Deposits." In *First Floridians and Last*
813 *Mastodons: The Page-Ladson Site in the Aucilla River*, edited by S. David Webb, 263–
814 331. Springer Netherlands. https://doi.org/10.1007/978-1-4020-4694-0_10.
815 Ngene, Shadrack, Moses Makonjio Okello, Joseph Mukeka, Shadrack Muya, Steve Njumbi, and
816 James Isiche. 2017. Home range sizes and space use of African elephants (*Loxodonta*
817 *africana*) in the Southern Kenya and Northern Tanzania borderland landscape.
818 International Journal of Biodiversity and Conservation 9(1): 9-26.
819 Nogués-Bravo, David, Jesús Rodríguez, Joaquín Hortal, Persaram Batra, and Miguel B. Araújo.
820 2008. "Climate Change, Humans, and the Extinction of the Woolly Mammoth." *PLOS*
821 *Biology* 6 (4): e79. https://doi.org/10.1371/journal.pbio.0060079.
822 Owen-Smith, R. Norman. 1992. *Megaherbivores: The Influence of Very Large Body Size on*
823 *Ecology*. Cambridge University Press.
824 Pacher, Martina, and Anthony J. Stuart. 2009. "Extinction Chronology and Palaeobiology of the
825 Cave Bear (Ursus Spelaeus)." *Boreas* 38 (2): 189–206. https://doi.org/10.1111/j.1502-

826 3885.2008.00071.x.
827 Pérez-Crespo, Víctor Adrián, Peter Schaaf, Gabriela Solís-Pichardo, Joaquín Arroyo-Cabrales,
828 Luis M. Alva-Valdivia, and José Ramón Torres-Hernández. 2016. "Strontium Isotopes
829 and Mobility of a Columbian Mammoth (Mammuthus Columbi) Population, Laguna de
830 Las Cruces, San Luis Potosí, México." *Geological Magazine* 153 (4): 743–49.
831 https://doi.org/10.1017/S001675681500103X.
832 Plumptre, A. J. 1994. "The Effects of Trampling Damage by Herbivores on the Vegetation of the
833 Pare National Des Volcans, Rwanda." *African Journal of Ecology* 32 (2): 115–29.
834 https://doi.org/10.1111/j.1365-2028.1994.tb00563.x.
835 Post, David M. 2002. "Using Stable Isotopes to Estimate Trophic Position: Models, Methods,
836 and Assumptions." *Ecology* 83 (3): 703–718. https://doi.org/10.1890/0012-
837 9658(2002)083[0703:USITET]2.0.CO;2.
838 Rabanus-Wallace, M. Timothy, Matthew Wooller, Grant Zazula, Elen Shute, A Hope Jahren,
839 Pavel Kosintsev, James Burns, James Breen, Bastien Llamas, and Alan Cooper. 2017.
840 Megafaunal isotopes reveal role of increase moisture on rangeland during late Pleistocene
841 extinctions. Nature Ecology and Evolution 1(0125). https://doi.org/10:1038/s41559-017-
842 0125.
843 Rasmussen, Sune O., Matthias Bigler, Simon P. Blockley, Thomas Blunier, Susanne L.
844 Buchardt, Henrik B. Clausen, Ivana Cvijanovic et al. 2014. A stratigraphic framework for
845 abrupt climatic changes during the Last Glacial period based on three synchronized
846 Greenland ice-core records: refining and extending the INTIMATE event stratigraphy.
847 *Quaternary Science Reviews* 106: 14-28.
848 Rhodes, A. N., J. W. Urbance, H. Youga, H. Corlew-Newman, C. A. Reddy, M. J. Klug, J. M.
849 Tiedje, and D. C. Fisher. 1998. "Identification of Bacterial Isolates Obtained from
850 Intestinal Contents Associated with 12,000-Year-Old Mastodon Remains." *Appl.*
851 *Environ. Microbiol.* 64 (2): 651–58.
852 Richards, M. P. and R. E. M. Hedges. 2003. Variations in bone collagen $\delta^{13}C$ and $\delta^{15}N$ values of
853 fauna from Northwest Europe over the last 40,000 years. Palaeogeography,
854 Palaeoclimatology, and Palaeoecology 193:261-267.
855 Ripple, William J., and Blaire Van Valkenburgh. 2010. "Linking Top-down Forces to the
856 Pleistocene Megafaunal Extinctions." *BioScience* 60 (7): 516–26.
857 https://doi.org/10.1525/bio.2010.60.7.7.
858 Rountrey, Adam N., Daniel C. Fisher, Alexei N. Tikhonov, Pavel A. Kosintsev, Pyotr A.
859 Lazarev, Gennady Boeskorov, and Bernard Buigues. 2012. "Early Tooth Development,
860 Gestation, and Season of Birth in Mammoths." *Quaternary International*, Mammoths and
861 Their Relatives 1: Biotopes, Evolution and Human Impact V International Conference,
862 Le Puy-en-Velay, 2010, 255 (March): 196–205.
863 https://doi.org/10.1016/j.quaint.2011.06.006.
864 Sah, S. P., H. Rita, and H. Ilvesniemi. 2006. "15N Natural Abundance of Foliage and Soil across
865 Boreal Forests of Finland." *Biogeochemistry* 80 (3): 277–288.
866 https://doi.org/10.1007/s10533-006-9023-9.
867 Saunders, Jeffrey J., Eric C. Grimm, Christopher C. Widga, G. Dennis Campbell, B. Brandon
868 Curry, David A. Grimley, Paul R. Hanson, Judd P. McCullum, James S. Oliver, and Janis
869 D. Treworgy. 2010. "Paradigms and Proboscideans in the Southern Great Lakes Region,
870 USA." *Quaternary International* 217 (1–2): 175–87.
871 https://doi.org/10.1016/j.quaint.2009.07.031.

872 Schubert, B. A., & Jahren, A. H. (2015). Global increase in plant carbon isotope fractionation
873 following the Last Glacial Maximum caused by increase in atmospheric p CO2. *Geology*,
874 43(5): 435-438.
875 Schulze, E.-D., F. S. Chapin, and G. Gebauer. 1994. "Nitrogen Nutrition and Isotope Differences
876 among Life Forms at the Northern Treeline of Alaska." *Oecologia* 100 (4): 406–12.
877 https://doi.org/10.1007/BF00317862.
878 Schwartz-Narbonne, R., F. J. Longstaffe, K. J. Kardynal, P. Druckenmiller, K. A. Hobson, C. N.
879 Jass, J. Z. Metcalfe, G. Zazula. 2019. "Reframing the mammoth steppe: Insights from
880 analysis of isotopic niches. *Quaternary Science Reviews* 215: 1-21.
881 Shearer, G, and D Kohl. 1993. "Natural Abundance of 15N: Fractional Contribution of Two
882 Sources to a Common Sink and Use of Isotope Discrimination." In *Nitrogen Isotope*
883 *Techniques*, 89–125. Academic Press.
884 Slater, Philip A., Kristin M. Hedman, and Thomas E. Emerson. 2014. "Immigrants at the
885 Mississippian Polity of Cahokia: Strontium Isotope Evidence for Population Movement."
886 *Journal of Archaeological Science* 44 (April): 117–27.
887 https://doi.org/10.1016/j.jas.2014.01.022.
888 Smith, Gregory James, and Larisa R. G. DeSantis. 2018. "Dietary Ecology of Pleistocene
889 Mammoths and Mastodons as Inferred from Dental Microwear Textures."
890 *Palaeogeography, Palaeoclimatology, Palaeoecology* 492 (March): 10–25.
891 https://doi.org/10.1016/j.palaeo.2017.11.024.
892 Stevens, Rhiannon, Roger Jacobi, Martin Street, Mietje Germonpre, Nicholas Conard, Susanne
893 Munzel, Robert E. M. Hedges. 2008. Nitrogen isotope analyses of reindeer (Rangifer
894 tarandus), 45,000 BP to 9,000 BP: Palaeoenvironmental reconstructions.
895 *Palaeogeography, Palaeoclimatology, Palaeoecology* 262: 32-45.
896 Stuart, A. J., P. A. Kosintsev, T. F. G. Higham, and A. M. Lister. 2004. "Pleistocene to Holocene
897 Extinction Dynamics in Giant Deer and Woolly Mammoth." *Nature* 431 (7009): 684.
898 https://doi.org/10.1038/nature02890.
899 Stuart, Anthony J., and Adrian M. Lister. 2011. "Extinction Chronology of the Cave Lion
900 Panthera Spelaea." *Quaternary Science Reviews*, Beringia and Beyond: Papers
901 Celebrating the Scientific Career of Andrei Vladimirovich Sher, 1939–2008, 30 (17):
902 2329–40. https://doi.org/10.1016/j.quascirev.2010.04.023.
903 ———. 2012. "Extinction Chronology of the Woolly Rhinoceros Coelodonta Antiquitatis in the
904 Context of Late Quaternary Megafaunal Extinctions in Northern Eurasia." *Quaternary*
905 *Science Reviews* 51 (September): 1–17. https://doi.org/10.1016/j.quascirev.2012.06.007.
906 Stuart, Anthony John. 2015. "Late Quaternary Megafaunal Extinctions on the Continents: A
907 Short Review." *Geological Journal* 50 (3): 338–63. https://doi.org/10.1002/gj.2633.
908 Surovell, Todd A., Spencer R. Pelton, Richard Anderson-Sprecher, and Adam D. Myers. 2016.
909 "Test of Martin's Overkill Hypothesis Using Radiocarbon Dates on Extinct Megafauna."
910 *Proceedings of the National Academy of Sciences* 113 (4): 886–91.
911 https://doi.org/10.1073/pnas.1504020112.
912 Surovell, Todd, Nicole Waguespack, and P. Jeffrey Brantingham. 2005. "Global Archaeological
913 Evidence for Proboscidean Overkill." *Proceedings of the National Academy of Sciences*
914 102 (17): 6231–36. https://doi.org/10.1073/pnas.0501947102.
915 Szpak, Paul, Darren R. Gröcke, Regis Debruyne, Ross D. E. MacPhee, R. Dale Guthrie, Duane
916 Froese, Grant D. Zazula, William P. Patterson, and Hendrik N. Poinar. 2010. "Regional
917 Differences in Bone Collagen $\delta^{13}C$ and $\delta^{15}N$ of Pleistocene Mammoths: Implications for

Paleoecology of the Mammoth Steppe." *Palaeogeography, Palaeoclimatology, Palaeoecology* 286 (1): 88–96. https://doi.org/10.1016/j.palaeo.2009.12.009.

Teale, Chelsea L., and Norton G. Miller. 2012. "Mastodon Herbivory in Mid-Latitude Late-Pleistocene Boreal Forests of Eastern North America." *Quaternary Research* 78 (1): 72–81. https://doi.org/10.1016/j.yqres.2012.04.002.

Tuross, Noreen, Marilyn L Fogel, and P. E Hare. 1988. "Variability in the Preservation of the Isotopic Composition of Collagen from Fossil Bone." *Geochimica et Cosmochimica Acta* 52 (4): 929–35. https://doi.org/10.1016/0016-7037(88)90364-X.

Uno, Kevin T., Jay Quade, Daniel C. Fisher, George Wittemyer, Iain Douglas-Hamilton, Samuel Andanje, Patrick Omondi, Moses Litoroh, and Thure E. Cerling. 2013. "Bomb-Curve Radiocarbon Measurement of Recent Biologic Tissues and Applications to Wildlife Forensics and Stable Isotope (Paleo)Ecology." *Proceedings of the National Academy of Sciences* 110 (29): 11736–41. https://doi.org/10.1073/pnas.1302226110.

Valeix, Marion, Hervé Fritz, Rodolphe Sabatier, Felix Murindagomo, David Cumming, and Patrick Duncan. 2011. "Elephant-Induced Structural Changes in the Vegetation and Habitat Selection by Large Herbivores in an African Savanna." *Biological Conservation* 144 (2): 902–12. https://doi.org/10.1016/j.biocon.2010.10.029.

Voelker, Steven L., Michael C. Stambaugh, Richard P. Guyette, Xiahong Feng, David a. Grimley, Steven W. Leavitt, Irina Panyushkina, et al. 2015. "Deglacial Hydroclimate of Midcontinental North America." *Quaternary Research* 83 (2): 336–344. https://doi.org/10.1016/j.yqres.2015.01.001.

Warinner, Christina, and Noreen Tuross. 2010. "Brief Communication: Tissue Isotopic Enrichment Associated with Growth Depression in a Pig: Implications for Archaeology and Ecology." *American Journal of Physical Anthropology* 141 (3): 486–493. https://doi.org/10.1002/ajpa.21222.

Widga, Chris, Stacey N. Lengyel, Jeffrey Saunders, Gregory Hodgins, J. Douglas Walker, and Alan D. Wanamaker. 2017a. "Late Pleistocene Proboscidean Population Dynamics in the North American Midcontinent." *Boreas* 46 (4): 772–82. https://doi.org/10.1111/bor.12235.

Widga, Chris, J. Douglas Walker, and Andrew Boehm. 2017b. "Variability in Bioavailable $^{87}Sr/^{86}Sr$ in the North American Midcontinent." *Open Quaternary* 3 (1): 4. https://doi.org/10.5334/oq.32.

Wolverton, Steve, R Lee Lyman, James H Kennedy, and Thomas W La Point. 2009. "The Terminal Pleistocene Extinctions in North America, Hypermorphic Evolution, and the Dynamic Equilibrium Model." *Journal of Ethobiology* 29 (1): 28–63. https://doi.org/10.2993/0278-0771-29.1.28.

Zazzo, Antoine, Marie Balasse, and William P. W.P. William P Patterson. 2006. "The Reconstruction of Mammal Individual History: Refining High-Resolution Isotope Record in Bovine Tooth Dentine." *Journal of Archaeological Science* 33 (8): 1177–1187. https://doi.org/10.1016/j.jas.2005.12.006.

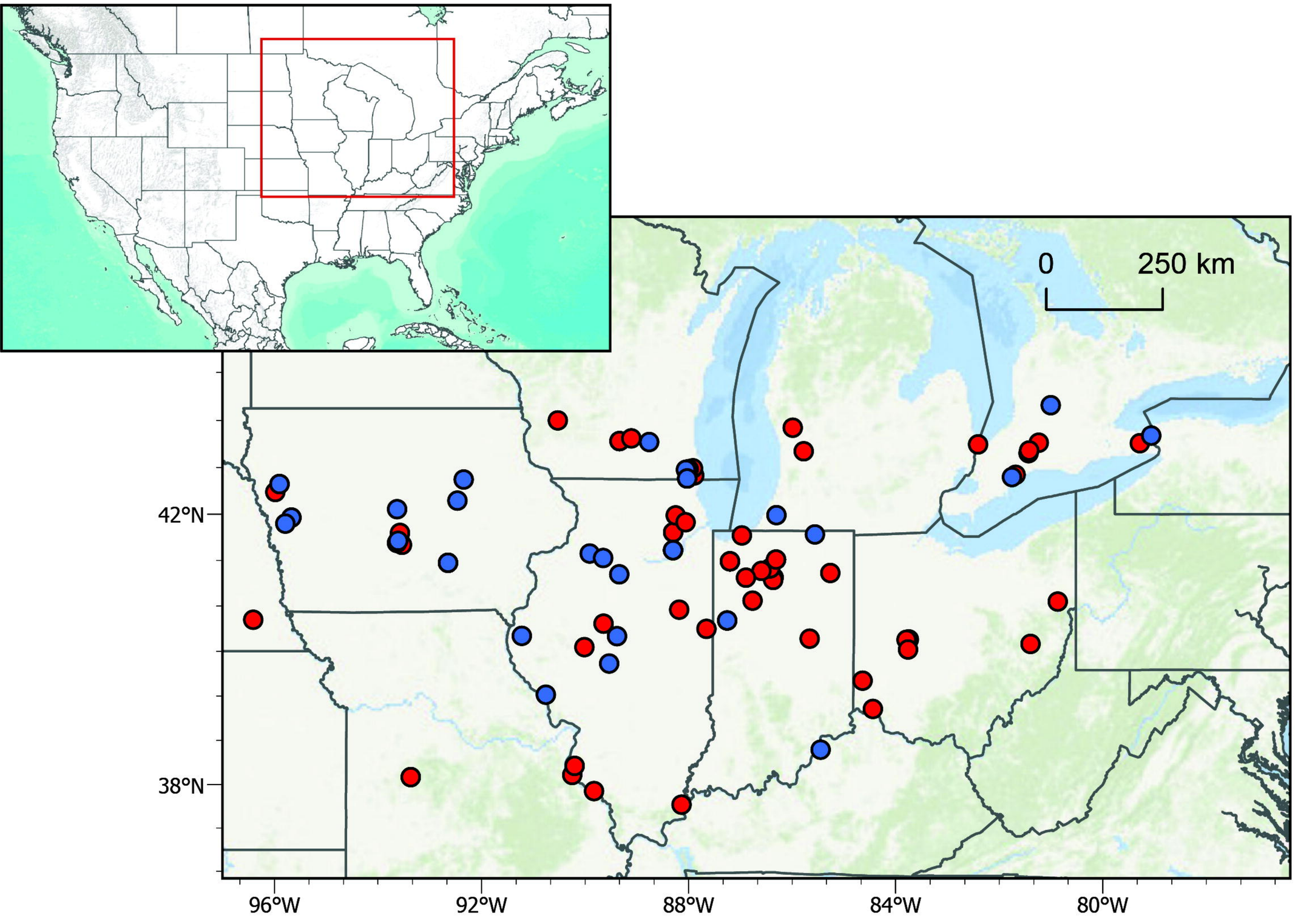

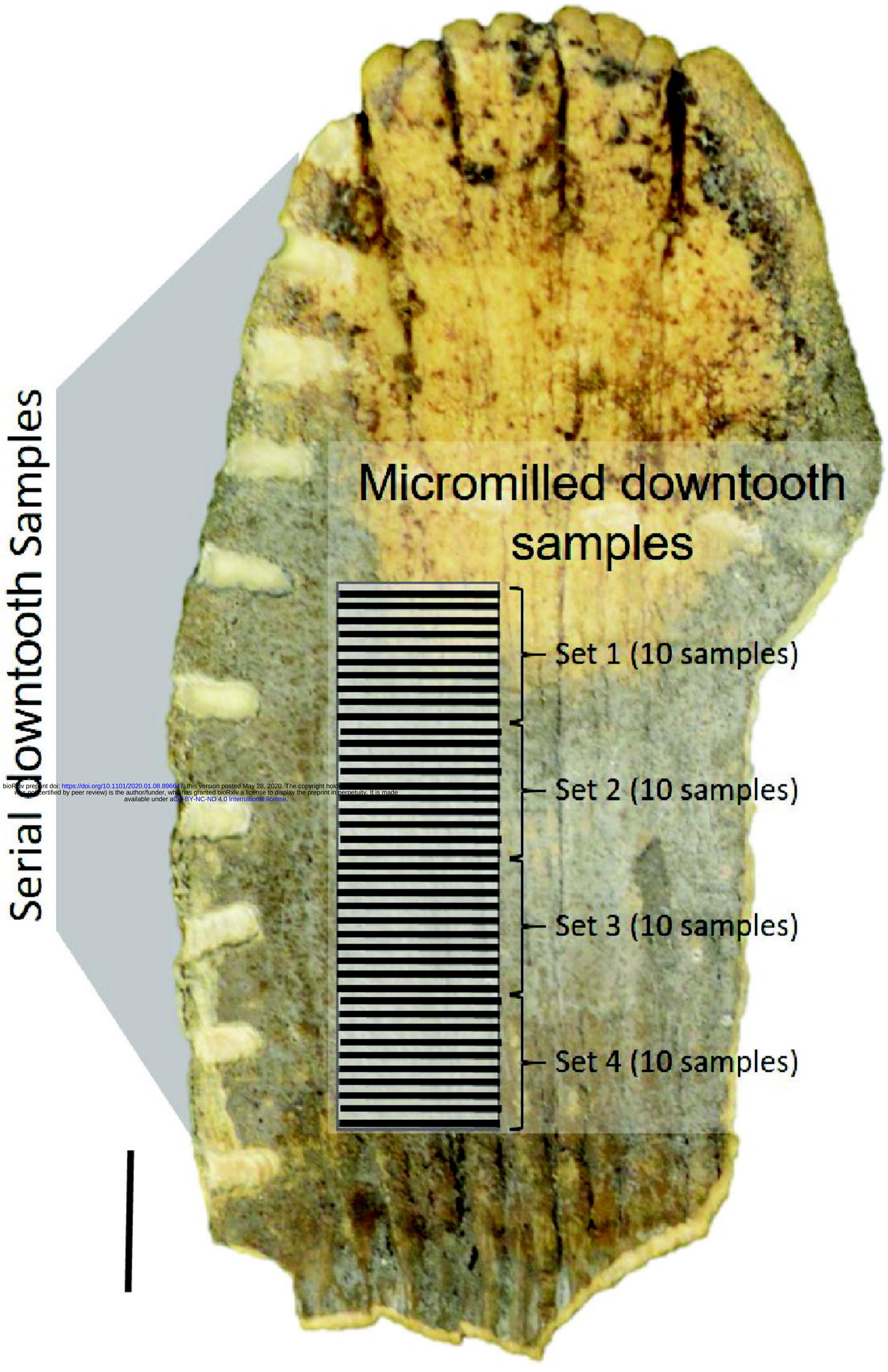

Cross Section of enamel sampling set showing milling depth.

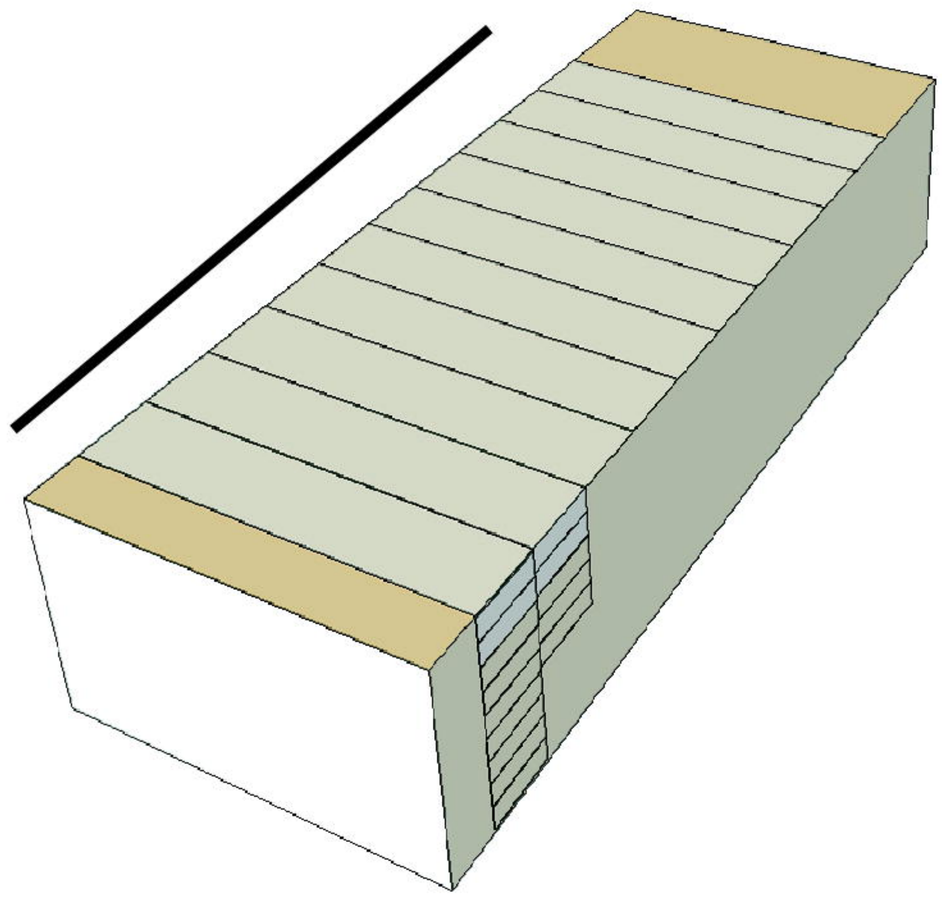

Enamel Sampling set.

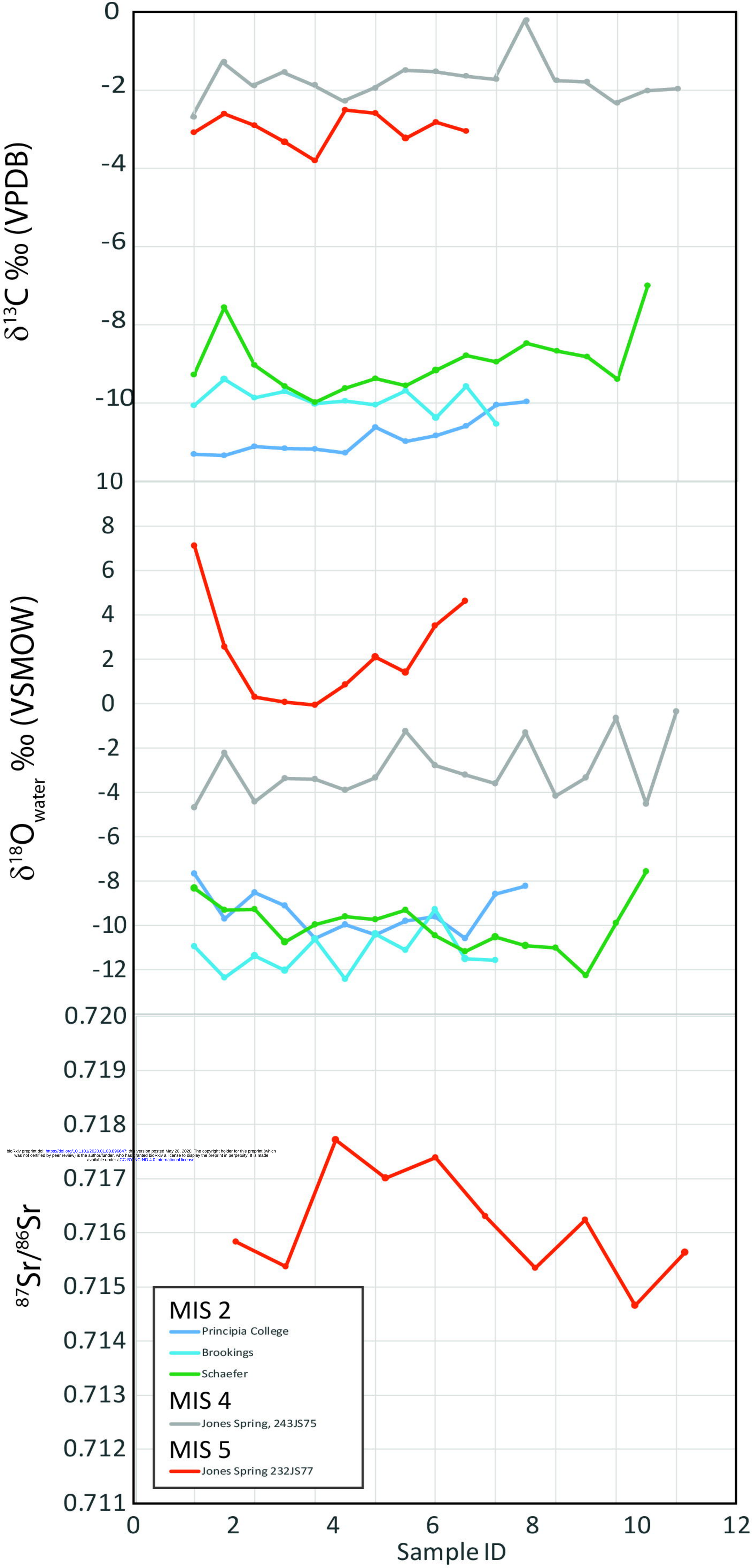

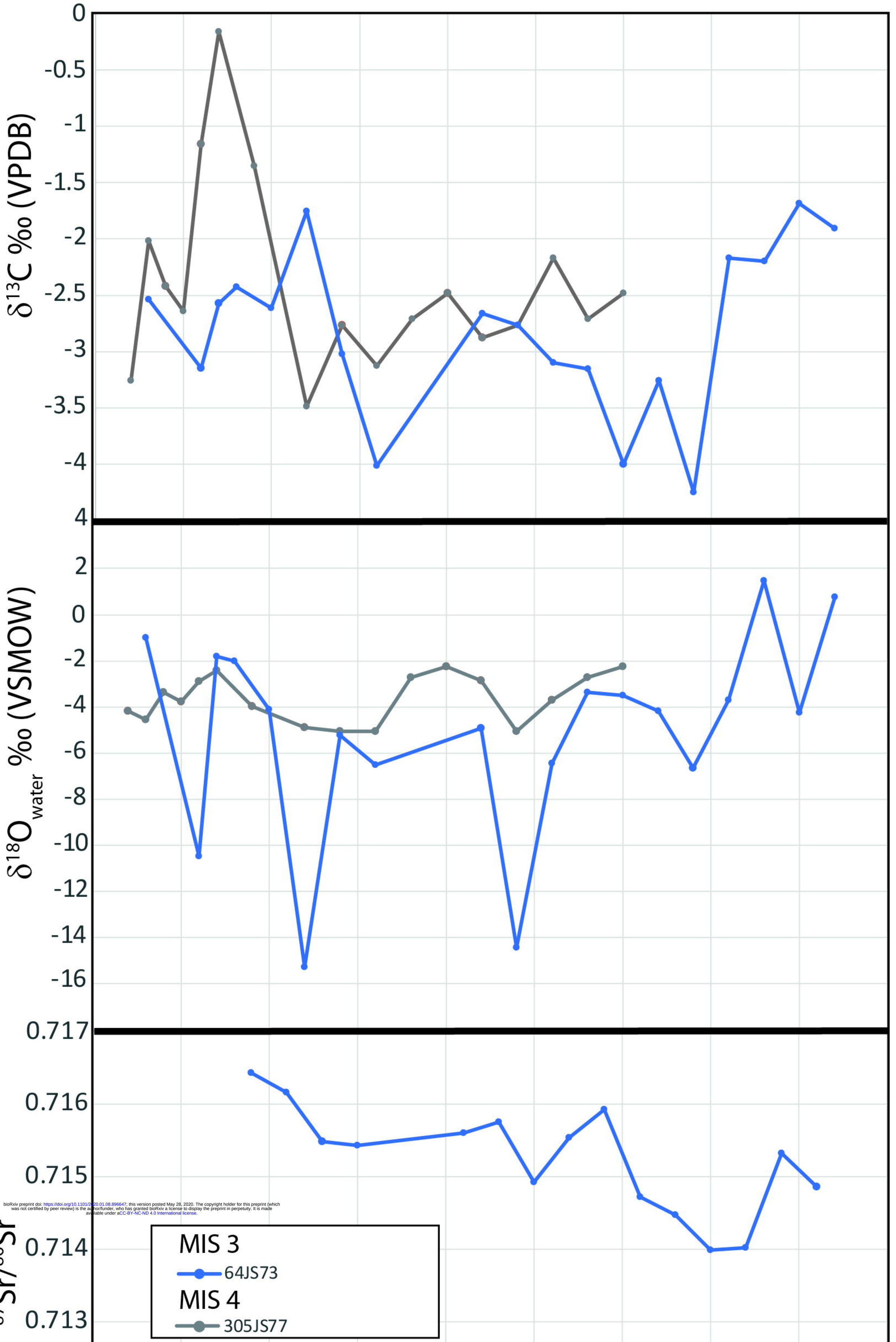

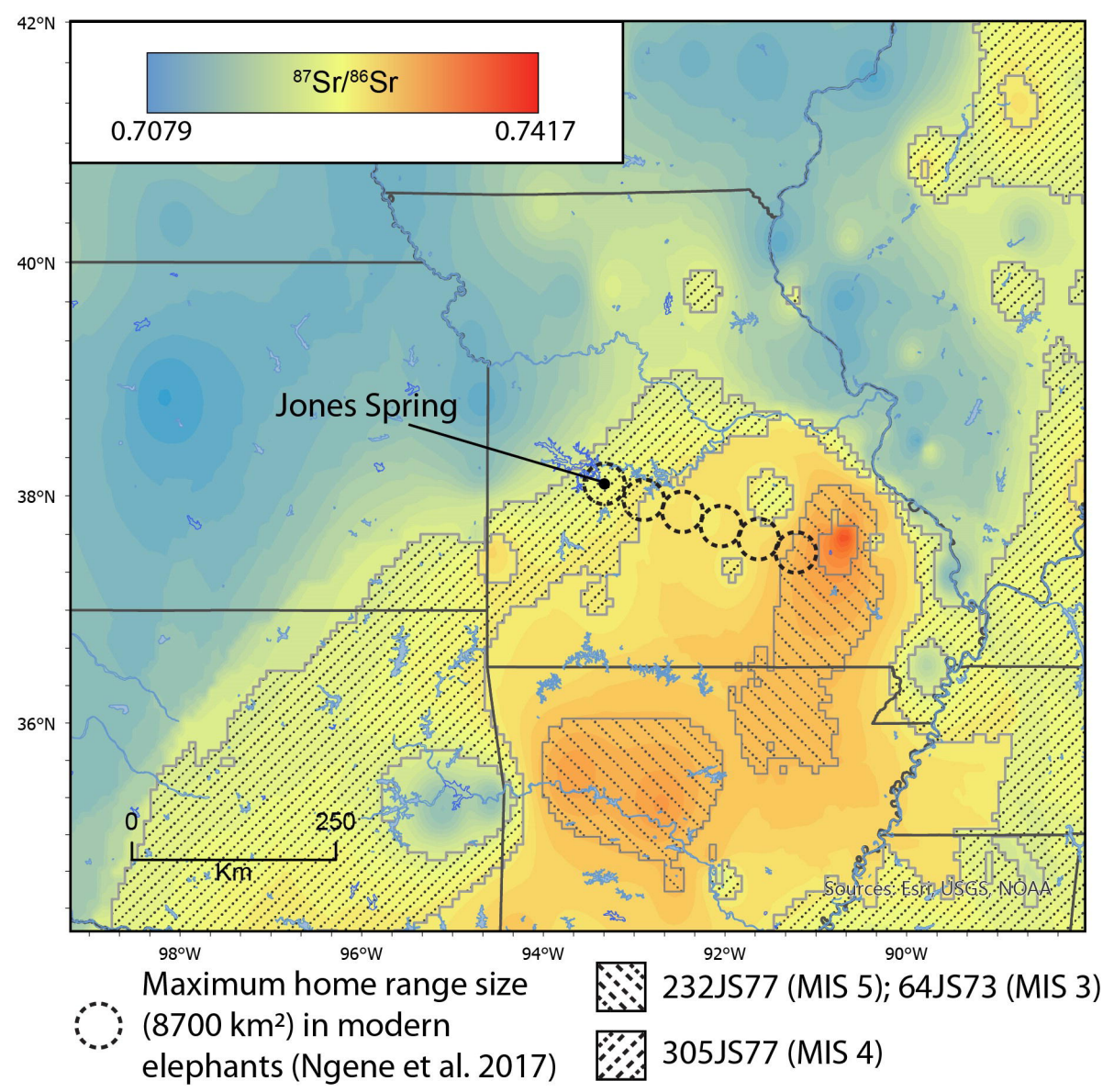
$^{87}Sr/^{86}Sr$
0.7079
0.7417
Jones Spring
42°N
40°N
38°N
36°N
0
250
Km
Sources: Esri, USGS, NOAA
98°W
96°W
94°W
92°W
90°W
Maximum home range size (8700 km²) in modern elephants (Ngene et al. 2017)
232JS77 (MIS 5); 64JS73 (MIS 3)
305JS77 (MIS 4)